COGITAO: A PROCEDURAL OBJECT-CENTRIC FRAME-WORK TO EVALUATE COMPOSITIONAL GENERALIZATION

Anonymous authors

000

001

002003004

005

006 007 008

010 011

012

013

014

015

016

017

018

019

021

023

024

027

029

031

033

035

036

037 038

040

041

042

045

Paper under double-blind review

ABSTRACT

The ability to compose learned concepts and apply them in novel settings is key to human intelligence, but remains a key challenge in state-of-the-art machine learning models. To address this issue, we introduce COGITAO, a modulable data-generation framework to evaluate compositional and systematic generalization in object-centric domains. Drawing inspiration from ARC-AGI's environment and problem-setting, COGITAO constructs rule-based tasks to be solved by applying a set of transformations to objects in grid-based environments. It supports composition over a set of 28 interoperable transformations, at adjustable composition-depth, along with extensive control over grid parametrization and object properties. This flexibility enables the creation of millions of unique task rules surpassing existing datasets by several orders of magnitude – across a broad range of difficulties, while allowing virtually unlimited sample generation per rule. Alongside open-sourcing our flexible data-generation framework, we release benchmark datasets and provide baseline results with several state-of-the-art architectures that incorporate inductive biases well-suited for compositionality, such as diffusion-based Transformers (LLaDA) or recurrent Transformers with Adaptive Computation Time (Universal Transformer/PonderNet). Despite strong in-domain performance, these models consistently fail to generalize to novel combinations of familiar elements – highlighting a persistent challenge in compositional and systematic generalization, which COGITAO allows to precisely characterize.

1 Introduction

Compositional and systematic generalization are core principles of human cognition (1). From a few examples of 'atomic' concepts, humans can later effortlessly combine these in exponentially many new ways and apply them in contexts far removed from those in which they were learned. As Lake and Baroni illustrate, "Once a person learns the meaning of a new verb 'dax,' they can immediately understand the meaning of 'dax twice' or 'sing and dax'" (2). Machine learning systems still struggle with these forms of generalization, making them a central research challenge (3; 4; 5; 6; 7; 8).

To foster progress in this direction, several benchmarks have been proposed, both in language (2; 9; 7; 10; 11) and vision (12; 13; 14; 15; 16; 17). Yet in vision, existing benchmarks lack the flexibility of their language counterparts: they provide limited control over compositional structure, offer a narrow range of tasks, and conflate visual complexity with relational structure – distracting from the essence of compositional generalization.

To close this gap, we introduce **CO**mpositional **G**eneralization **In** Transformations **And O**bjects: **COGITAO** – a procedural object-centric framework designed to generate simple, controllable datasets to probe compositional and systematic generalization in an abstract visual domain. Our generator's strength stems from its capacity to compose freely, at arbitrary compositional depth, a set of 28 atomic transformations –

thus enabling to create millions of unique transformation sequences, with a virtually infinite amount of task samples, across a wide range of difficulties.

In our COGITAO framework, models can learn to apply a given sequence of object-transformations and generate an 'output grid' given an 'input grid' and a transformation sequence (see Figure 1). Furthermore, models can be implemented in various environment configurations (e.g., with different numbers or types of objects, or grid dimensions).

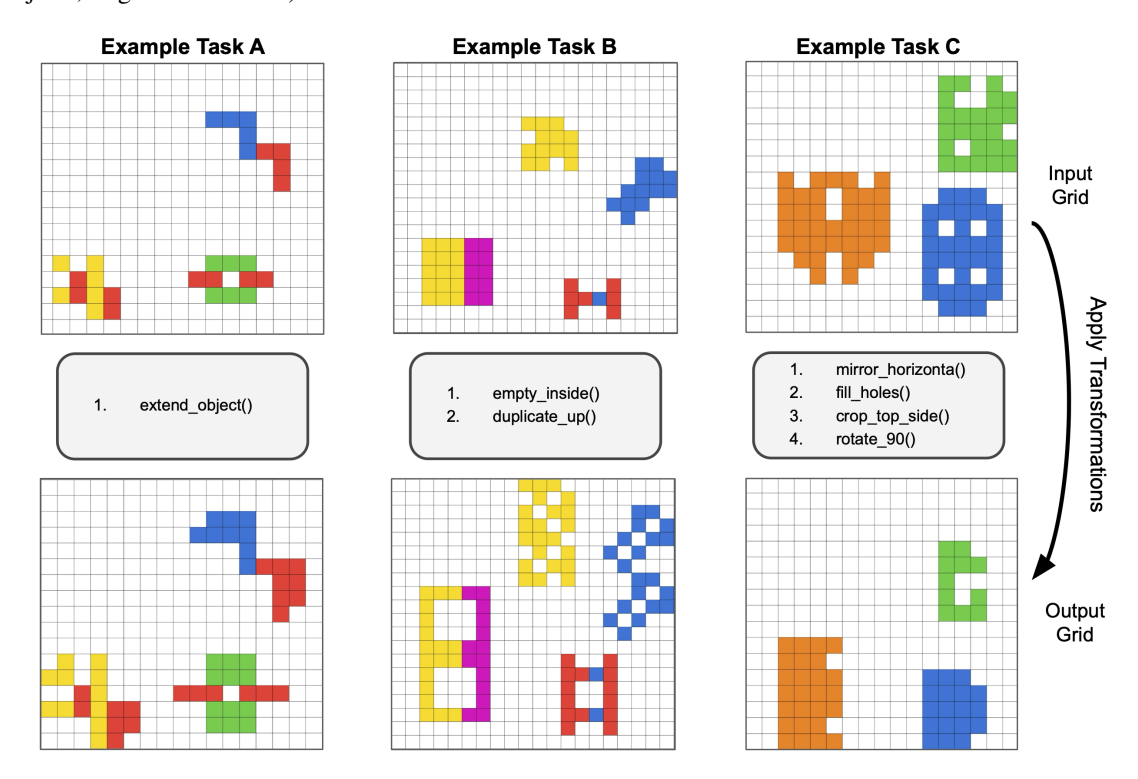


Figure 1: Set of input-output pair examples from our COGITAO generator, with input grids on top rows, and corresponding output grids (after transforming input) on the bottom rows. Each input-output pair follows a different transformation sequence (see boxes on middle row) and a given grid/object parametrization.

The key test of compositionality comes from varying transformation sequences and environment parameters between training and testing time. Analogous to the linguistic example "dax twice" or "sing and dax" (2), a model trained to "rotate" objects once should generalize to "rotate twice" or "rotate and translate," provided it has seen the individual rotate and translate transformations during training.

COGITAO is deliberately abstract and synthetic, which enables to precisely isolate core compositional reasoning from confounding visual complexity. Despite its simplicity and grid-based nature, it captures compositional and systematic generalization in ways essential for real-world vision tasks. Indeed, the object-centric, order-dependent operations exemplified in COGITAO— such as selectively modifying or relocating objects while preserving the surrounding scene — mirror the challenges studied in robotics (18) and world-model research (19; 20; 21; 22). We therefore position COGITAO not only as a static image benchmark, but also as an image-and-action framework that explicitly links perception to interaction (see Appendix A). To facilitate transfer to natural vision, COGITAO additionally offers RGB renderings of its tasks to train standard computer-vision models (see Appendix B), while preserving all its diagnostic power.

To demonstrate our framework's utility and support further research, we release a suite of benchmark datasets built from different COGITAO configurations. We train state-of-the-art architectures that incorporate inductive biases well suited for systematic and compositional generalization (Diffusion Transformers (23) and Pondering Looped Transformers (24; 25)). We also compare to baseline Transformers (optionally infused with object-centric inductive biases (26) and ResNet (27). Our experiments intentionally target the raw inductive biases of well-specified architectures rather than large foundation models, whose training data and precise design details often remain opaque ¹. Despite solid in-domain performance, we report that these models consistently fail to generalize to novel combinations of familiar visual elements. Our findings highlight the need for architectures that move beyond pattern matching and memorization (28; 29; 30; 31) towards truly structured, compositional understanding – COGITAOprovides a simple framework to foster progress in this direction.

In this paper, our main contributions are:

- 1. We introduce COGITAO: a procedural, grid-based and object-centric framework that freely composes 28 atomic object-transformations to generate millions of unique, controllable input—output rules at adjustable composition depth.
- 2. We extend COGITAO beyond simple grids to RGB renderings for real-world vision transfer, and from single input—output pairs to sequences of images and actions for world-model research.
- 3. We create and release multiple benchmark datasets targeting specific aspects of compositional and systematic generalization, enabling reproducible and scalable experimentation.
- 4. We provide cohesive baselines with state-of-the-art models known for their reasoning capabilities, and show that they consistently fail to generalize to out-of-distribution compositions highlighting the open challenge of systematic compositional generalization in object-centric domains.

2 RELATED WORK

Our proposed framework builds upon prior research in compositional and systematic generalization – applied to both language and vision data. While these areas are often interconnected, we find that compositional generalization benchmarks in the visual domain lag behind their language counterpart in and flexibility and scope. This is mainly due to the difficulty of procedurally generating visual data of adequate task fidelity compared to language-like data.

Compositional Generalization in Language Several datasets and benchmarks have enabled targeted focus on systematic and compositional generalization in deep learning architectures for natural language processing. The SCAN dataset (2) is most akin to our work – it consists of commands mapped to action sequences. Models must compose commands, both within and outside the training distribution, to execute them correctly. Our dataset is similar to SCAN in that it contains various experimental settings in which the difference between training and testing distribution varies (across primitives, combinations, or sequence length). Several works have shown that models can achieve good performance on SCAN with specific architectures, representation methods, or data augmentation techniques (32; 33; 34; 35; 30), as well as different training strategies such as meta-learning (6), but there is still no consensus on the best architecture for compositional tasks. Analogous to Scan, COGS (10) or PCFG (11) also leverage a modular language to construct compositional tasks. In a similar but more formal spirit, the CFQ dataset (7) is designed to maximize compound divergence while minimizing atomic divergence between train and test sets, which the authors argue is an optimal setting to study compositional generalization. Our approach follows this logic, as primitive elements are shared,

¹We note that by evaluating Transformers and Diffusion based models, we cover the architectures of most foundation models.

but their combinations differ between training and test time. Other datasets reproduce this logic in other sequential modalities, such as within the SQL language (36) or mathematical reasoning (37).

Compositional Generalization in Vision Compositional generalization in vision is often studied in pairs with visual reasoning, which has gained significant traction in recent years. Most aligned to our work are benchmarks such as ARC-AGI (38), Raven's Progressive Matrices (39), and Procedurally Generated Matrices (14), which use handcrafted shapes and environments to simplify visual processing in light of reasoning. With similar handcrafted shapes and environments, but with a more targeted focus on compositional and systematic generalization as opposed to reasoning, we find other important datasets such as dSprites (40), CLEVR (12), Compositional Visual Reasoning (13), SVRT (15), and SVIB (41). These datasets are all built out of procedurally generated shapes with varying properties (e.g., color, size, texture) and make use of different types of rules, as well as composition of properties to evaluate models' compositional capabilities and object-centric representations. Most aligned with our objectives are the CVR (13) and SYGAR (16) datasets. CVR targets compositional visual relations in an odd-one-out classification format, whereas SYGAR requires grid prediction but adopts the Meta-Learning (MLC) framework (6) and does not providing clear benchmarks. Both are more limited in scope and compositional and environmental control compared to COGITAOOther datasets, such as CATER (17), contrary to the aforementioned datasets which use procedurally generated shapes, focus on compositional generalization in the real-world visual domain. However, we believe these inevitably conflate compositional reasoning ability with visual complexity, preventing a focused study on compositional generalization.

3 COGITAO GENERATOR

Our motivation stemmed from attempting to make progress at the original ARC challenge (38). Similar to the authors of conceptARC (42), we observed that the data regime of the ARC-AGI was too small (low data availability), too diverse (high variance between individual tasks) to make sound scientific progress on some of the abilities crucial to the challenge and lacking from modern deep learning approaches. While other researchers adopted the path of scale, big-data regime and novel inference-time methods such as test-time-training and chain of thoughts reasoning to tackle the challenge (43; 44; 45), we chose instead to follow a more principled approach, as this allows us to directly evaluate the capabilities of raw architectures and inductive biases to compose and generalize on basic sets of problems. As such, we designed a generator tailored to gauge the systematic and compositional generalization abilities of models, specifically through composing object-centric transformations. Our primary tasks consist of rule-based input-output pairs, where each rule is defined by applying a sequence of transformations to objects arranged on grids of variable sizes. This setup enables the creation of a wide spectrum of tasks with a large difficulty range. Our framework becomes valuable when varying the transformation sequences and environment parametrizations between training and testing sets – which is how we propose to gauge models' compositional. Specifically, we control systematic and compositional generalization along two axes:

- **Compositional Generalization**: COGITAO enables the composition of multiple object transformations at various levels of depth (i.e., the number of transformations applied sequentially) through a set of 28 primitive transformations (e.g., translations, rotations, and mirroring).
- Environmental Generalization: COGITAO allows control over additional parameters to assess the generalization capabilities of models, i.e., their ability to apply learned transformations in varied environments. Users can modify the number of objects per grid, the complexity, size, and color of shapes, and the grid size, enabling the generation of different environment versions between training and testing phases.

Both axes of research are also enabled through our RGB rendering and sequential rendering, which are respectively introduced in appendix B and A. While we view these two extensions as essential for future

development in natural vision and World-Model research, the main manuscript focuses primarily on the simpler, grid-based input-transformation-output framework.

3.1 Generator Overview

COGITAO Objects: COGITAO samples from a collection of 23,000 pre-generated objects varying in size, shape, symmetry, connectivity, and color pattern. Each object uses pixel colors 1–9 (0 is reserved for the background) and is placed to avoid overlap and contact with other objects, ensuring clear boundaries between them (see C.1 for details).

COGITAO Transformations: We provide a set of 28 simple object-transformations (such as translations, padding, duplicating.. see C.2. Each transformation was crafted to respect two core rules: 1) each transformation should be composable with all other transformations, and 2) each transformation should modify the object in a way that should not be systematically equivalent to a combination of other transformations. Rule 1 is critical to ensure that our generator maximizes the number of possible tasks that can be generated and avoids degenerate cases. Rule 2 avoids redundancy in the transformations (see Appendix C.2 for details). We ensure each transformation is individually learnable by all models used for training (see D for further details).

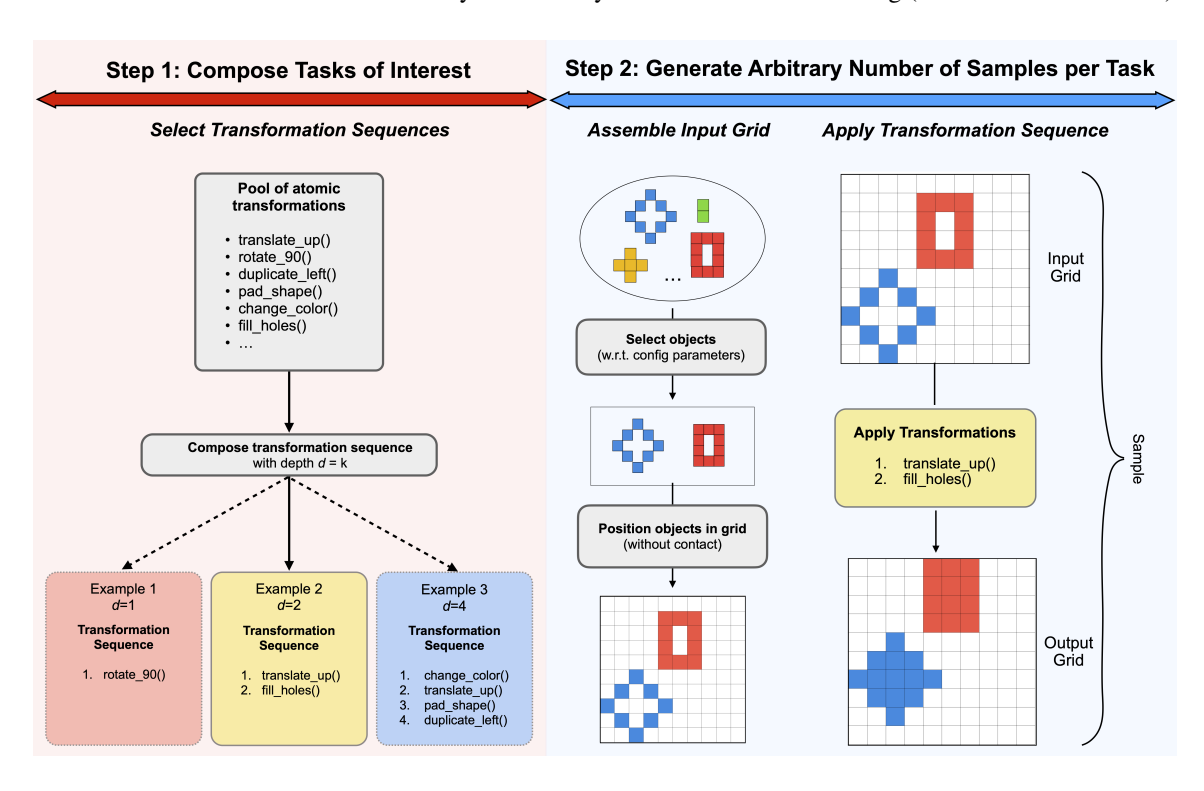


Figure 2: COGITAO is a Python-based procedural and object-centric data generator, inspired by the ARC-AGI (38) grid-based environment. COGITAO samples transformation sequences, then, given the configuration requested by the user and the sampled transformations, randomly samples and position objects in an input grid. Once objects are positioned in the input grid, each transformation is sequentially applied to each object.

236 a 237 ra 238 a 239 n 240 tr 241 F 242 c 243 n 244 P

COGITAO Generation The generator can either randomly sample a sequence of transformations from a specified pool or use a user-defined sequence. After selecting the transformation sequence, it assembles random objects (w.r.t. config parameters) on the input grid, allowing each transformation to be applied to an output grid. Because some transformations (e.g., cropping) are irreversible and certain combinations are non-commutative, the order of transformations matters. With 28 available transformations and a maximum transformation depth k, the theoretical upper bound on the number of distinct tasks is $N=n_{\rm transforms}^k=28^k$. For example, at dept d=5 and an adequate number of objects and grid size, the generator could theoretically create $n_{\rm tasks}=28^5\approx 1.7\times 10^8$ unique tasks. Provided the grid is sufficiently large and generation time is not a limiting factor, the depth of compositional transformations can be arbitrarily large, making the space of possible tasks effectively unbounded. Further details on the generation method can be found in C.3.

4 EXPERIMENTS

To illustrate the utility of the COGITAO generator, we designed a set of benchmark experiments that highlight its potential for studying compositional and systematic generalization in the visual domain. These experiments define the *initial* benchmark for the community to beat, while also serving as illustrative examples –COGITAO can generate far richer and more challenging tasks than those presented here. In the Discussion section, we outline additional configurations and encourage researchers to explore this broader task space once the current benchmark is mastered.

4.1 EXPERIMENT DETAILS

We outline two "studies" - one focusing on the composition of transformations, the **Compositional Generalization** (*CompGen*) study, and the other on environment variations (with fixed transformation sequence): the **Environmental Generalization** (*EnvGen*) study. In each case, we measure the capacity of models to perform tasks that differ in some way from the tasks seen during training — either with respect to transformation composition in the *CompGen* study or with respect to environment parametrization in the *EnvGen* study.

For both studies, we define different *experiment settings* which focus on different aspects of compositional and systematic generalization. For each *experiment setting* we create 5 "experiments" - these are different instances of the *experiment settings* in which we only vary the transformation sequences. This is to ensure that the results we report are robust across different transformation combinations (e.g., translation-based transformation sequences might be easier than rotation-based ones - see Appendix D).

For each experiment, we train on 100,000 unique training samples, and test on two unique and distinct sets of 1,000 samples; one test-set follows the same distribution (i.e., in-domain (ID) set) as the training set, and the other is out-of-distribution (OOD), from which we evaluate generalization.

In the *CompGen* study, we train and test a model on multiple transformation sequences within a single experiment. This contrasts with the *EnvGen* study, where models are trained on only a single transformation per experiment. To handle this complexity, we provide context that indicates to the model which sequence to perform. We do so by appending a task embedding to the input sequence, similar to the approach in CVR (13). This embedding is a sequence of tokens that specifies the transformations in the correct order. For example, the task "translate_up-rotate_90" would have an embedding like ['T', 'R'], while the inverse task "rotate_90-translate_up" would be ['R', 'T']. For OOD testing, the models may be evaluated on new or longer sequences of these transformations. However, every individual token would have been seen during training.

We provide below an outline of each experiment setting for each of our two studies, and refer the reader to the Appendix E for more details.

² 'Adequate' refers to grid and object configurations that avoid frequent generation failures—for instance, attempting to place ten objects in a 5×5 grid while performing four object transformations is impractical.

CompGen - Compositional Generalization

- C1 Atomic + Composite → Unseen Composite: Train on atomic (depth 1) and composite (depth 2) tasks; test on unseen depth 2 composites built out of the same atomic transformations (tf.) as training.
- C2 Restricted Composite → Unseen Composite: Train only on a subset of composites (depth 2); test on unseen depth 2 composites built out of the same atomic as training.
- C3 Atomic + Composite → Deeper Composite: Train on atomic and depth 2 composites; test on depth 3 composites built out of the same atomics as training.

EnvGen - Environmental Generalization

- G1 More Objects: Train with 1–2 objects; test with 3–4 objects (fixed grid size and object complexity).
- G2 Larger Grids: Train on 10×10–15×15 grids; test on 16×16–20×20 grids (fixed object number and complexity).
- G3 Larger Objects: Train on objects sized 1×1–5×5; test on objects sized 6×6–10×10 (fixed grid size and number of objects).
- *G4 More Complex Objects*: Train on symmetric, single-colored objects; test on asymmetric, multi-colored (fixed grid size and number of objects).
- G5 Combined: Train on simple cases (1–2 objects, 10×10–15×15 grids, symmetric single-colored 1×1–5×5 objects); test on all harder variants simultaneously (3-4 objects, 16x16-20x20 grids, multi-colored asymmetric objects).

4.2 Models

We evaluate four encoder architectures, each paired with a two-layer MLP head for grid tokens classification. All models are of comparable size (approximately 1 million parameters) to ensure a fair evaluation. Empirically, increasing the model size did not substantially improve generalization.

- Vanilla TF: We use a standard Vanilla Transformer (TF)(46) with learned absolute positional encodings (47). Vision transformers are considered state-of-the-art for vision tasks and offer a strong baseline for COGITAO tasks.
- **Grid TF**: To better capture the structure of grid-based reasoning tasks, we introduce a Grid TF, an adapted version of ViTARC (26) that incorporates task-specific biases: object positional encoding (OPE) (26), PEMixer modules (26), register tokens (48), and modified positional encoding schemes (49; 50). These additions are designed to support spatial reasoning over structured grid-based data.
- **Pondering Looped TF (PL-TF)**: Based on PonderNet (24; 25), we evaluate a Transformer architecture that incorporates recurrence through iterative weight sharing and adaptive computation time. This architecture aims to reflect an inductive bias towards iterative reasoning and composition through multi-step transformations, making it particularly well suited for compositional tasks.
- LLaDA: In addition to vision-like and grid-specific architectures, as well as models with a recurrent architecture, we investigate the performance of language models. Specifically, we evaluate LLaDA (23), a diffusion-based language model yielding state-of-the-art performance on symbolic and logical tasks.

The selected models encompass a diverse set of architectural paradigms based on the current state-of-the-art in both vision and sequence modeling. This selection is designed to address the heterogeneous computational requirements of abstract visual reasoning tasks and spans a wide spectrum of modeling characteristics, thus providing baselines for COGITAO. Comprehensive architectural details are provided in Appendix F.

4.3 Training

All models are trained³ from scratch using supervised learning. For each experiment, we evaluate and test in-domain (ID) and out-of-domain (OOD) data. We aim to train all models as similar as possible to have a fair comparison among them. The models are trained for 10 epochs (except for LLaDA, which is trained for 20 epochs, as on average 50% of the tokens are masked). We select the best models based on their performance on the validation OOD split before evaluating them on the test sets.

All models are trained using the AdamW optimizer (51) with a linear warm-up for 200 steps, followed by cosine annealing of the learning rate. We use a batch size of 64 for training and 50 for evaluation and testing. Further training details for all models are provided in Appendix G.

4.4 EXPERIMENT RESULTS

To provide robust empirical baselines for the COGITAObenchmark and to systematically evaluate the compositional and generalization capabilities of different model architectures, we apply the baseline models to the three CompGen settings (C1-C3) and the five EnvGen settings (G1-G5) described in Section 4.1.

Table 4.4 provides an overview of the results across these settings, reporting both in-domain (ID) and out-of-domain (OOD) grid accuracy. Grid accuracy is defined as the percentage of samples for which the predicted grid structure matches the ground truth exactly (i.e., the entire grid is predicted correctly). Performance values are averaged across 5 variations of the experiment setting (i.e., different transformation sequences - see E for more details) with 3 seeds each.

	Vanilla-TF		Grid-TF		PL-TF			LLaDA				
ES	ID	OOD	Δ	ID	OOD	Δ	ID	OOD	Δ	ID	OOD	Δ
C1	16.5	0.0	16.5	59.8	0.0	59.8	81.0	0.1	80.9	44.9	0.0	44.9
C2	17.8	0.0	17.8	68.5	0.0	68.5	79.0	0.1	78.9	46.2	0.0	46.2
C3	29.4	4.0	25.4	63.3	8.3	55.0	82.0	7.2	74.8	84.1	7.8	76.3
G1	98.4	78.9	19.5	99.3	90.1	9.2	93.8	85.5	8.3	99.5	90.1	9.4
G2	82.0	2.1	79.9	98.0	77.0	21.0	92.6	54.9	37.6	98.5	62.4	36.1
G3	57.6	22.5	35.1	85.0	26.6	58.4	92.0	27.2	64.8	82.4	26.8	55.6
G4	46.2	21.8	24.4	86.9	19.0	67.9	86.8	37.5	49.3	81.3	32.0	49.3
G5	72.5	0.0	72.5	95.0	0.2	94.8	80.7	8.9	71.8	70.0	10.1	60.0

Table 1: Performance of models on experiments across experiment settings (ES) of the main studies. We report the ID (in-domain) and OOD (out-of-domain) results for test grid accuracy (i.e., % of perfect matches) and the ID to OOD relative drop Δ averaged over all experiments within the experiment setting.

The experimental results reveal several key trends (Table 4.4). Grid-TF, our grid-specialized transformer, provides strong in-domain (ID) accuracy across most settings and remains the most stable baseline overall - particularly in the *EnvGen* study. However, the PL-TF model consistently matches or surpasses Grid-TF in several critical out-of-domain (OOD) tests. In the *CompGen* study, PL-TF attains the best ID accuracy in C1 and C2 and competitive OOD performance in C3. It is the only model that solves a task on C1 and C2 OOD. Within the *EnvGen* settings, PL-TF delivers the best OOD scores in G3 (27.2) and G4 (37.5), and strong ID results in G3–G4, indicating improved robustness to object scale and complexity changes. LLaDA

³Training of the Vanilla and Grid-TF models was performed using an NVIDIA GeForce RTX 3090 GPU. Training of PL-TF was performed on NVIDIA A100 GPU. Training of LLaDA used an NVIDIA V100 GPU.

remains a strong performer, achieving the highest OOD accuracy in G1 and competitive results in G2 and G5,. Vanilla-TF, by contrast, performs pooly, with sharp ID–OOD drops across nearly all tasks. Overall, these findings underscore both the difficulty of the COGITAO benchmark and the promise of PL-TF's architectural choices for compositional and environmental generalization, while confirming that no current model fully solves the challenge.

5 DISCUSSION

Summary COGITAO offers a controlled and targeted framework for studying compositional and systematic generalization, specifically in object-centric environments. With millions of possible tasks and abundant training samples, COGITAO provides an unmatched degree of compositional control in abstract visual domains. By leveraging simple grid-based environments and object-centric transformations, it enables isolating core compositional capabilities while avoiding the visual and data complexity of more naturalistic datasets. Indeed, our core hypothesis is that models that cannot exhibit compositional generalization in this controlled, simple and abstract environment are unlikely to succeed in the far noisier and less structured settings of real-world vision. Nevertheless, to bridge the gap to real-world vision, we provide an RGB extension to COGITAO onto which both the *CompGen* and *EnvGen* benchmarks can be applied.

Unlike classification-based benchmarks such as CVR (13), RPM (39), SVRT (15), and PGM (14), our generator requires models to *generate* output grids - a real test of compositional understanding. It aligns more closely with challenges like ARC-AGI (38) and its successors (52; 16; 42; 53). We also extend our input-output generation framework to a sequential framework (Appendix A), with set of frames and object-centric "actions", thus making it highly relevant sequential manipulation tasks.

In our benchmark experiments, we evaluate Vanilla TF, Grid TF, Pondering Looped TF, and LLaDA across the COGITAO tasks. These models were chosen to represent the state-of-the-art in vision and sequence modeling, including both general-purpose and grid-specialized architectures. While they provide a diverse and strong baseline, future work should explore additional architectures. The experiments reveal a consistent trend: while these models perform well on in-domain tasks, they fail dramatically in out-of-distribution scenarios requiring compositional understanding. In our *CompGen* study, while models learned to learn ID transformations sequences, they all failed when faced with unseen OOD transformation sequences. Similarly, *EnvGen* performance degrades significantly with increased task complexity. These results support growing evidence that current state-of-the-art sequence and vision models rely heavily on pattern recognition rather than systematic compositional reasoning (29). COGITAO provides a controlled environment to diagnose these fundamental limitations and guide the development of more robust, generalizable architectures and inductive biases.

Future Work COGITAO offers a compelling platform for driving progress in compositional generalization, and it supports several promising research directions. First, extending the framework to *in-context learning*, for example, by providing demonstration examples, could allow evaluation of generalization in settings known to benefit from longer contexts (44), particularly in large foundation models (54; 55; 56). Second, due to its controllable environment and adjustable difficulty, COGITAO is well-suited for *curriculum learning*, where task complexity is gradually increased to guide learning. Third, analyzing *internal model representations* trained on COGITAO may reveal whether and how models develop object-centric or transformation-centric abstractions.

Outlook Mastering the existing hardest COGITAO settings would be a significant milestone toward genuinely compositional architectures. More so - doing so using only generator-produced data would show that a model can identify primitive operations, apply them sequentially, and recombine them in novel settings – akin to a core human cognition (1)

6 REPRODUCIBILITY STATEMENT

We have made every effort to ensure that our results are fully reproducible. Detailed descriptions of the COGITAO generator, object creation process, and transformation suite are provided in Sections 3–4 of the main paper, with additional implementation details, algorithmic pseudo-code, and full experimental settings in Appendix 7–9. All training hyper-parameters, model architectures, and evaluation procedures are explicitly specified (Sections 4.1–4.4 and Appendix 8–9). To facilitate independent verification, we release the complete source code and data generation framework as anonymous supplementary material, with the same version available at our GitHub repository ⁴. The benchmark datasets used in our experiments can be reproduced or directly accessed via HuggingFace. These resources include scripts to regenerate all figures, tables, and experimental results reported in the paper.

REFERENCES

- [1] Jerry A. Fodor and Zenon W. Pylyshyn. Connectionism and cognitive architecture: A critical analysis. *Cognition*, 28(1-2):3–71, March 1988.
- [2] Brenden Lake and Marco Baroni. Generalization without Systematicity: On the Compositional Skills of Sequence-to-Sequence Recurrent Networks. In *The 35th International Conference on Machine Learning* (ICML), volume 80 of *Proceedings of Machine Learning Research*, pages 2873–2882. PMLR, July 2018.
- [3] Lukas Galke, Yoav Ram, and Limor Raviv. Deep neural networks and humans both benefit from compositional language structure. *Nature Communications*, 15(1):10816, December 2024.
- [4] Tarek R. Besold and Ute Schmid. Why Generality Is Key to Human-Level Artificial Intelligence. *Advances in Cognitive Systems*, 4:13–24, 2016.
- [5] Thaddäus Wiedemer, Prasanna Mayilvahanan, Matthias Bethge, and Wieland Brendel. Compositional Generalization from First Principles. In *Advances in Neural Information Processing Systems (NeurIPS)*, volume 36, pages 6941–6960. Curran Associates, Inc., 2023.
- [6] Brenden M. Lake and Marco Baroni. Human-like systematic generalization through a meta-learning neural network. *Nature*, 623(7985):115–121, 2023.
- [7] Daniel Keysers, Nathanael Schärli, Nathan Scales, Hylke Buisman, Daniel Furrer, Sergii Kashubin, Nikola Momchev, Danila Sinopalnikov, Lukasz Stafiniak, Tibor Tihon, Dmitry Tsarkov, Xiao Wang, Marc van Zee, and Olivier Bousquet. Measuring Compositional Generalization: A Comprehensive Method on Realistic Data. In *The 8th International Conference on Learning Representations (ICLR)*, 2020.
- [8] Zhenlin Xu, Marc Niethammer, and Colin A Raffel. Compositional Generalization in Unsupervised Compositional Representation Learning: A Study on Disentanglement and Emergent Language. In Advances in Neural Information Processing Systems (NeurIPS), volume 35, pages 25074–25087. Curran Associates, Inc., 2022.
- [9] Simon Schug, Seijin Kobayashi, Yassir Akram, Maciej Wolczyk, Alexandra Maria Proca, Johannes von Oswald, Razvan Pascanu, Joao Sacramento, and Angelika Steger. Discovering modular solutions that generalize compositionally. In *The 12th International Conference on Learning Representations (ICLR)*, 2024.

⁴Code is available at the following URL: https://anonymous.4open.science/r/COGITAO-4E72

- [10] Najoung Kim and Tal Linzen. COGS: A Compositional Generalization Challenge Based on Semantic Interpretation. In *The 2020 Conference on Empirical Methods in Natural Language Processing* (EMNLP), pages 9087–9105. Association for Computational Linguistics, 2020.
 - [11] Dieuwke Hupkes, Verna Dankers, Mathijs Mul, and Elia Bruni. Compositionality decomposed: How do neural networks generalise? *Journal of Artificial Intelligence Research*, 67:757–795, 2020.
 - [12] Justin Johnson, Bharath Hariharan, Laurens van der Maaten, Li Fei-Fei, C. Lawrence Zitnick, and Ross Girshick. CLEVR: A Diagnostic Dataset for Compositional Language and Elementary Visual Reasoning. In *The IEEE Conference on Computer Vision and Pattern Recognition (CVPR)*, July 2017.
 - [13] Aimen Zerroug, Mohit Vaishnav, Julien Colin, Sebastian Musslick, and Thomas Serre. A Benchmark for Compositional Visual Reasoning. In *Advances in Neural Information Processing Systems (NeurIPS)*, volume 35, pages 29776–29788. Curran Associates, Inc., 2022.
 - [14] David Barrett, Felix Hill, Adam Santoro, Ari Morcos, and Timothy Lillicrap. Measuring abstract reasoning in neural networks. In *The 35th International Conference on Machine Learning (ICML)*, volume 80 of *Proceedings of Machine Learning Research*, pages 511–520. PMLR, July 2018.
 - [15] François Fleuret, Ting Li, Charles Dubout, Emma K. Wampler, Steven Yantis, and Donald Geman. Comparing machines and humans on a visual categorization test. *Proceedings of the National Academy of Sciences*, 108(43):17621–17625, October 2011.
 - [16] Philipp Mondorf, Shijia Zhou, Monica Riedler, and Barbara Plank. Enabling systematic generalization in abstract spatial reasoning through meta-learning for compositionality. arXiv preprint arXiv:2504.01445, 2025.
 - [17] Rohit Girdhar and Deva Ramanan. Cater: A diagnostic dataset for compositional actions and temporal reasoning. *arXiv preprint arXiv:1910.04744*, 2019.
 - [18] Deb Roy, Kai-Yuh Hsiao, and Nikolaos Mavridis. Mental imagery for a conversational robot. *IEEE Transactions on Systems, Man, and Cybernetics, Part B (Cybernetics)*, 34(3):1374–1383, 2004.
 - [19] David Ha and Jürgen Schmidhuber. World models. arXiv preprint arXiv:1803.10122, 2(3), 2018.
 - [20] Danijar Hafner, Jurgis Pasukonis, Jimmy Ba, and Timothy Lillicrap. Mastering diverse domains through world models. *arXiv preprint arXiv:2301.04104*, 2023.
 - [21] Jake Bruce, Michael D Dennis, Ashley Edwards, Jack Parker-Holder, Yuge Shi, Edward Hughes, Matthew Lai, Aditi Mavalankar, Richie Steigerwald, Chris Apps, et al. Genie: Generative interactive environments. In *Forty-first International Conference on Machine Learning*, 2024.
 - [22] Stefano Ferraro, Pietro Mazzaglia, Tim Verbelen, and Bart Dhoedt. Focus: object-centric world models for robotic manipulation. *Frontiers in Neurorobotics*, 19:1585386, 2025.
 - [23] Shen Nie, Fengqi Zhu, Zebin You, Xiaolu Zhang, Jingyang Ou, Jun Hu, Jun Zhou, Yankai Lin, Ji-Rong Wen, and Chongxuan Li. Large Language Diffusion Models. *arXiv preprint arXiv:2502.09992*, 2025. Version Number: 2.
 - [24] Andrea Banino, Jan Balaguer, and Charles Blundell. Pondernet: Learning to ponder. *arXiv preprint* arXiv:2107.05407, 2021.
 - [25] Mostafa Dehghani, Stephan Gouws, Oriol Vinyals, Jakob Uszkoreit, and Łukasz Kaiser. Universal transformers, 2019.

- [26] Wenhao Li, Yudong Xu, Scott Sanner, and Elias Boutros Khalil. Tackling the Abstraction and Reasoning Corpus with Vision Transformers: the Importance of 2D Representation, Positions, and Objects. arXiv preprint arXiv:2410.06405, 2024. Version Number: 1.
 - [27] Kaiming He, Xiangyu Zhang, Shaoqing Ren, and Jian Sun. Deep Residual Learning for Image Recognition. In *The IEEE Conference on Computer Vision and Pattern Recognition (CVPR)*, pages 770–778, Las Vegas, NV, USA, June 2016. IEEE.
 - [28] Dzmitry Bahdanau, Shikhar Murty, Michael Noukhovitch, Thien Huu Nguyen, Harm de Vries, and Aaron Courville. Systematic generalization: what is required and can it be learned? *arXiv preprint arXiv:1811.12889*, 2018.
 - [29] Robert Geirhos, Jörn-Henrik Jacobsen, Claudio Michaelis, Richard Zemel, Wieland Brendel, Matthias Bethge, and Felix A. Wichmann. Shortcut learning in deep neural networks. *Nature Machine Intelligence*, 2(11):665–673, November 2020.
 - [30] Róbert Csordás, Kazuki Irie, and Juergen Schmidhuber. The devil is in the detail: Simple tricks improve systematic generalization of transformers. *arXiv* preprint arXiv:2108.12284, 2021.
 - [31] Nouha Dziri, Ximing Lu, Melanie Sclar, Xiang (Lorraine) Li, Liwei Jiang, Bill Yuchen Lin, Sean Welleck, Peter West, Chandra Bhagavatula, Ronan Le Bras, Jena Hwang, Soumya Sanyal, Xiang Ren, Allyson Ettinger, Zaid Harchaoui, and Yejin Choi. Faith and Fate: Limits of Transformers on Compositionality. In *Advances in Neural Information Processing Systems (NeurIPS)*, volume 36, pages 70293–70332. Curran Associates, Inc., 2023.
 - [32] Roberto Dessì and Marco Baroni. CNNs found to jump around more skillfully than RNNs: Compositional Generalization in Seq2seq Convolutional Networks. In *The 57th Annual Meeting of the Association for Computational Linguistics (ACL)*, pages 3919–3923, Florence, Italy, 2019. Association for Computational Linguistics.
 - [33] Jacob Andreas. Good-Enough Compositional Data Augmentation. In *The 58th Annual Meeting of the Association for Computational Linguistics (ACL)*, pages 7556–7566. Association for Computational Linguistics, 2020.
 - [34] Michal Auersperger and Pavel Pecina. Solving SCAN Tasks with Data Augmentation and Input Embeddings. In *The International Conference on Recent Advances in Natural Language Processing (RANLP)*, pages 86–91. INCOMA Ltd., September 2021.
 - [35] João Loula, Marco Baroni, and Brenden Lake. Rearranging the Familiar: Testing Compositional Generalization in Recurrent Networks. In *The 2018 EMNLP Workshop BlackboxNLP: Analyzing and Interpreting Neural Networks for NLP*, pages 108–114, Brussels, Belgium, 2018. Association for Computational Linguistics.
 - [36] Catherine Finegan-Dollak, Jonathan K. Kummerfeld, Li Zhang, Karthik Ramanathan, Sesh Sadasivam, Rui Zhang, and Dragomir Radev. Improving Text-to-SQL Evaluation Methodology. In *The 56th Annual Meeting of the Association for Computational Linguistics (ACL)*, volume 1, pages 351–360, Melbourne, Australia, 2018. Association for Computational Linguistics.
 - [37] David Saxton, Edward Grefenstette, Felix Hill, and Pushmeet Kohli. Analysing Mathematical Reasoning Abilities of Neural Models. In *The 7th International Conference on Learning Representations (ICLR)*, 2019.
 - [38] François Chollet. On the Measure of Intelligence. *arXiv preprint arXiv:1911.01547*, 2019. Version Number: 2.

- [39] John and Jean Raven. Raven Progressive Matrices. In *Handbook of Nonverbal Assessment*, pages 223–237. Springer US, Boston, MA, 2003.
 - [40] Christopher P. Burgess, Loic Matthey, Nicholas Watters, Rishabh Kabra, Irina Higgins, Matt Botvinick, and Alexander Lerchner. MONet: Unsupervised Scene Decomposition and Representation. *arXiv* preprint arXiv:1901.11390, 2019. Version Number: 1.
 - [41] Yeongbin Kim, Gautam Singh, Junyeong Park, Caglar Gulcehre, and Sungjin Ahn. Imagine the Unseen World: A Benchmark for Systematic Generalization in Visual World Models. In *The 27th Conference on Neural Information Processing Systems (NeurIPS): Datasets and Benchmarks Track*, 2023.
 - [42] Arsenii Kirillovich Moskvichev, Victor Vikram Odouard, and Melanie Mitchell. The ConceptARC Benchmark: Evaluating Understanding and Generalization in the ARC Domain. *Transactions on Machine Learning Research (TMLR)*, 2023.
 - [43] Ryan Greenblatt. Getting 50% (SOTA) on ARC-AGI with GPT-4o, June 2024.
 - [44] Jack Cole and Mohamed Osman. Don't Throw the Baby Out With the Bathwater: How and Why Deep Learning for ARC, March 2025.
 - [45] François Chollet. OpenAI o3 Breakthrough High score on ARC-AGI-Pub, December 2024.
 - [46] Alexey Dosovitskiy, Lucas Beyer, Alexander Kolesnikov, Dirk Weissenborn, Xiaohua Zhai, Thomas Unterthiner, Mostafa Dehghani, Matthias Minderer, Georg Heigold, Sylvain Gelly, Jakob Uszkoreit, and Neil Houlsby. An Image is Worth 16x16 Words: Transformers for Image Recognition at Scale. In *The 9th International Conference on Learning Representations (ICLR)*, 2021.
 - [47] Ashish Vaswani, Noam Shazeer, Niki Parmar, Jakob Uszkoreit, Llion Jones, Aidan N Gomez, Ł ukasz Kaiser, and Illia Polosukhin. Attention is All you Need. In *Advances in Neural Information Processing Systems (NeurIPS)*, volume 30. Curran Associates, Inc., 2017.
 - [48] Timothée Darcet, Maxime Oquab, Julien Mairal, and Piotr Bojanowski. Vision Transformers Need Registers. In *The 12th International Conference on Learning Representations (ICLR)*, 2024.
 - [49] Peter Shaw, Jakob Uszkoreit, and Ashish Vaswani. Self-Attention with Relative Position Representations. In *The 2018 Conference of the North American Chapter of the Association for Computational Linguistics (NAACL): Human Language Technologies*, volume 2, pages 464–468, New Orleans, Louisiana, 2018. Association for Computational Linguistics.
 - [50] Jianlin Su, Murtadha Ahmed, Yu Lu, Shengfeng Pan, Wen Bo, and Yunfeng Liu. RoFormer: Enhanced transformer with Rotary Position Embedding. *Neurocomputing*, 568:127063, February 2024.
 - [51] Ilya Loshchilov and Frank Hutter. Decoupled Weight Decay Regularization. In *The 7th International Conference on Learning Representations (ICLR)*, 2019.
 - [52] Michael Hodel. Addressing the Abstraction and Reasoning Corpus via Procedural Example Generation. *arXiv preprint arXiv:2404.07353*, 2024. Version Number: 1.
 - [53] Rim Assouel, Pau Rodriguez, Perouz Taslakian, David Vazquez, and Yoshua Bengio. Object-centric Compositional Imagination for Visual Abstract Reasoning. In ICLR 2022 Workshop on the Elements of Reasoning: Objects, Structure and Causality, 2022.
 - [54] Shengnan An, Zeqi Lin, Qiang Fu, Bei Chen, Nanning Zheng, Jian-Guang Lou, and Dongmei Zhang. How Do In-Context Examples Affect Compositional Generalization? In *The 61st Annual Meeting of the Association for Computational Linguistics (ACL)*, volume 1, pages 11027–11052, Toronto, Canada, 2023. Association for Computational Linguistics.

- [55] Xingxuan Zhang, Haoran Wang, Jiansheng Li, Yuan Xue, Shikai Guan, Renzhe Xu, Hao Zou, Han Yu, and Peng Cui. Understanding the Generalization of In-Context Learning in Transformers: An Empirical Study. In *The 13th International Conference on Learning Representations (ICLR)*, 2025.
 - [56] Andrew K. Lampinen, Arslan Chaudhry, Stephanie C. Y. Chan, Cody Wild, Diane Wan, Alex Ku, Jörg Bornschein, Razvan Pascanu, Murray Shanahan, and James L. McClelland. On the generalization of language models from in-context learning and finetuning: a controlled study. *arXiv* preprint arXiv:2505.00661, 2025. Version Number: 2.
 - [57] Sergey Ioffe and Christian Szegedy. Batch normalization: Accelerating deep network training by reducing internal covariate shift, 2015.
 - [58] Abien Fred Agarap. Deep learning using rectified linear units (relu), 2019.
 - [59] Qiang Wang, Bei Li, Tong Xiao, Jingbo Zhu, Changliang Li, Derek F. Wong, and Lidia S. Chao. Learning deep transformer models for machine translation, 2019.
 - [60] Ruibin Xiong, Yunchang Yang, Di He, Kai Zheng, Shuxin Zheng, Chen Xing, Huishuai Zhang, Yanyan Lan, Liwei Wang, and Tie-Yan Liu. On layer normalization in the transformer architecture, 2020.
 - [61] Dan Hendrycks and Kevin Gimpel. Gaussian error linear units (gelus), 2023.
 - [62] Ofir Press, Noah A. Smith, and Mike Lewis. Train short, test long: Attention with linear biases enables input length extrapolation, 2022.
 - [63] Francesco Locatello, Dirk Weissenborn, Thomas Unterthiner, Aravindh Mahendran, Georg Heigold, Jakob Uszkoreit, Alexey Dosovitskiy, and Thomas Kipf. Object-Centric Learning with Slot Attention. In Advances in Neural Information Processing Systems (NeurIPS), volume 33, pages 11525–11538. Curran Associates, Inc., 2020.
 - [64] Khashayar Gatmiry, Nikunj Saunshi, Sashank J. Reddi, Stefanie Jegelka, and Sanjiv Kumar. Can looped transformers learn to implement multi-step gradient descent for in-context learning?, 2024.
 - [65] Angeliki Giannou, Shashank Rajput, Jy yong Sohn, Kangwook Lee, Jason D. Lee, and Dimitris Papailiopoulos. Looped transformers as programmable computers, 2023.
 - [66] Liu Yang, Kangwook Lee, Robert Nowak, and Dimitris Papailiopoulos. Looped transformers are better at learning learning algorithms, 2024.
 - [67] Biao Zhang and Rico Sennrich. Root Mean Square Layer Normalization. In *Advances in Neural Information Processing Systems (NeurIPS)*, volume 32. Curran Associates, Inc., 2019.
 - [68] Stefan Elfwing, Eiji Uchibe, and Kenji Doya. Sigmoid-weighted linear units for neural network function approximation in reinforcement learning. *Neural Networks*, 107:3–11, November 2018.

A SEQUENTIAL-COGITAO

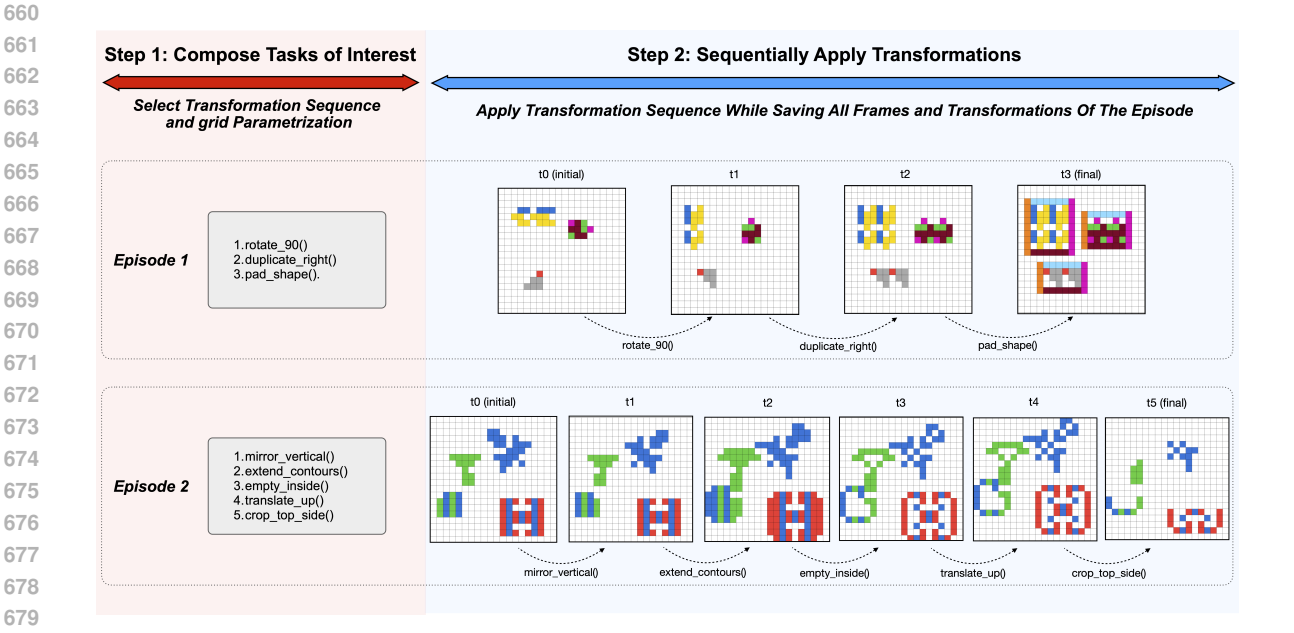


Figure 3: Overview of Sequential-COGITAO. Episodes of are generated from an initially sampled transformation sequence and grid parametrization. Each individual frame is saved, along with its corresponding transformations. We note that transitions for each individual objects are also available, but not shown here for visualization constraints.

Standard COGITAO tasks present a single input grid and expect a model to generate the final output after a composed transformation sequence. Sequential COGITAO extends this by exposing every intermediate state in the transformation chain. Instead of training solely on start—end pairs, models must either predict each intermediate grid or reason over an explicit temporal trajectory of transformations. This is particularly relevant for World Model research (19), where applying action to objects while preserving the environment is of particular importance (20; 21; 22). Both *CompGen* and *EnvGen* methodologies can seamlessly be applied to Sequential-COGITAO (also in a RGB rendering - see B) - enabling targeted and compositionality-focused research on perception and interaction tasks - a needed addition to the field.

B RGB RENDERING OF COGITAO

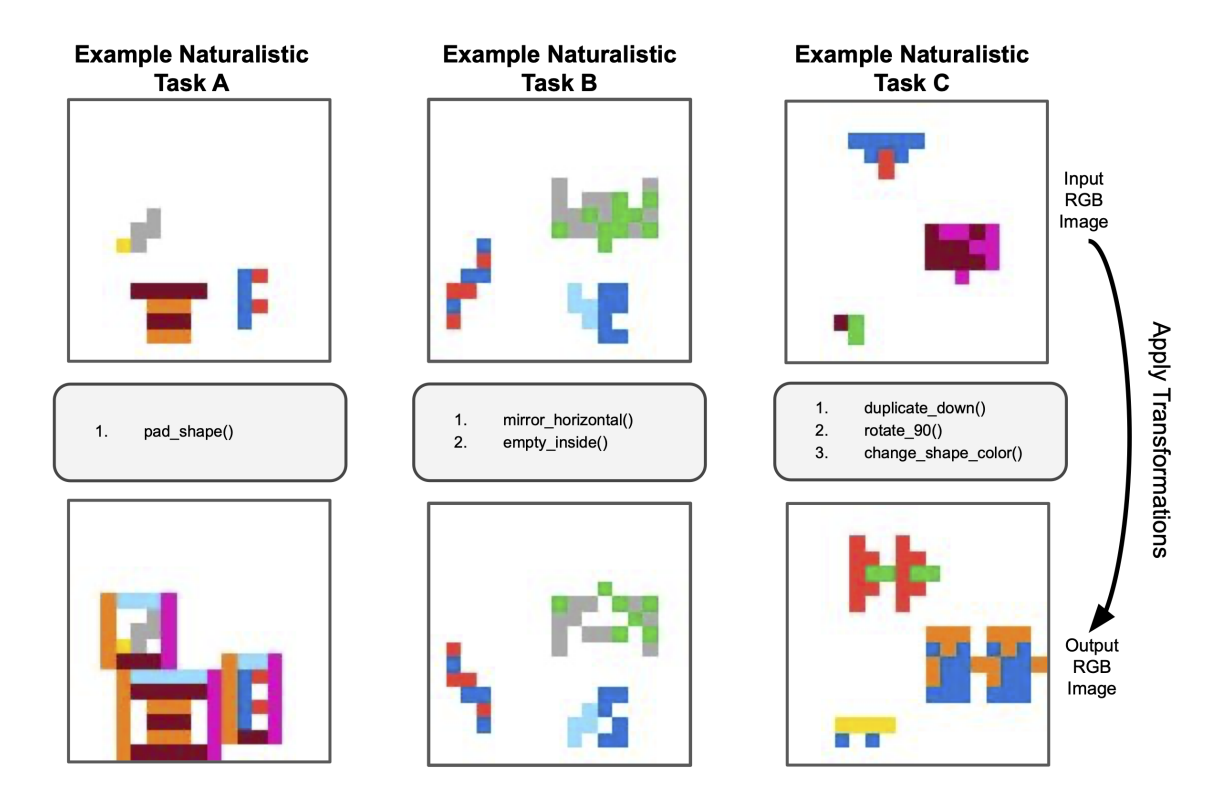


Figure 4: Set of input-output pair examples from our RGB rendering of COGITAO with input *images* on top rows, and corresponding output *images* (after transforming input) on the bottom rows. The images are 128x128x3, saved as .jpeg. Gray borders are added for visualization purposes only - they are not present on the images. Note: Objects are purposely blurry to outline their RGB nature - crisper rendering are straightforward.

To assess how compositional generalization persists beyond synthetic grids, we introduce COGITAO-RGB, a rendering of the benchmark in standard RGB images. Each sample is a 128 × 128 RGB image (configurable if desired) in which the discrete grid visualization is removed and objects are drawn on a plain white (or black) background. We convert the benchmark datasets presented in 4.1 to this format, excluding G1-2 and G1-5 where variable grid sizes are essential; G1-1, G1-3, and G1-4 translate directly. All 28 transformations from §C.2 remain fully applicable, but models must now infer object location and scale without explicit grid cues, increasing perceptual difficulty. Generation and train/test splits follow the original procedure. COGITAO-RGB thus bridges abstract grid worlds and natural image statistics, enabling researchers to test whether compositional and systematic generalization tested in the grid setting carries over to more realistic visual conditions.

C FURTHER DETAILS ON COGITAO CORE GENERATOR

C.1 COGITAO OBJECTS

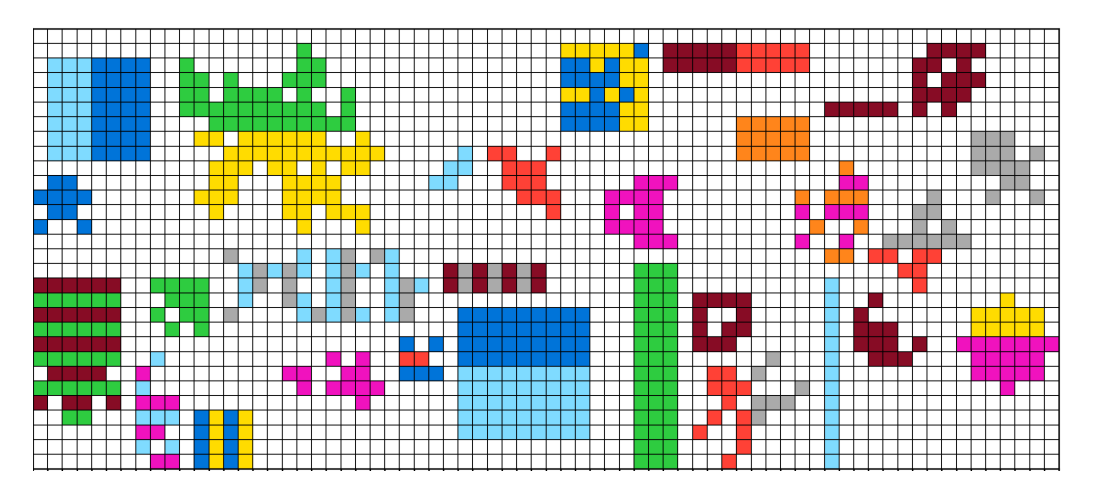


Figure 5: Random example of generated objects. The objects are generated with a variety of properties, including size, symmetry, connectivity, colors, color patterns, and footprints. Note: objects are not allowed to overlap, touch, or be inside one another in our generator environment, as reflected in the above image.

Rather than generating objects on the fly, which can be more costly computationally, we favour a method where we pre-generate a large set of 23000 object, and compute a table of properties or that these objects satisfy. This allows us to efficiently sort through objects at generation time with-respect-to the constraints specified by the user, as well as the object constraints that the transformation suite may impose. We share the file with these objects along with our code release, as well as the code used to generate these, so the community can expand the number of objects at will. Below, are all the properties through which we iterate, creating combination of every single parameter, up until a max object dimension of 15x15 pixels.

- Size: Number of rows, columns, and pixels.
- **Symmetry**: Horizontal, vertical, diagonal, point, and no symmetry.
- Connectivity: "4 connected" (only connected through adjacent edges), "8 connected" (only connected through adjacent or diagonal edges), or even "distance" (object can be composed of unconnected blocks).
- Colors: Single colored or multi-colored.
- Color Pattern: Uniform (single color), column stripes, row stripes, diagonal stripes, top-bottom coloring (object split in two colors), right-left coloring (object split in two colors), or random.
- Footprints: Predefined objects such as Rectangle, disk, square, diamond, or ellipse.

C.2 COGITAO TRANSFORMATIONS

We provide a set of 28 object-transformations, which the community can further expand. As noted in the main manuscript, each transformation was chosen to respect two core rules: 1) each transformation should be composable with all other transformations, and 2) each transformation should modify the object in a way that should not be systematically equivalent to a combination of other transformations. Rule 1 is critical to ensure that our generator maximizes the number of possible tasks that can be generated and

800

801

802

803

804

805

806 807

808

809

810

811 812

813

814

815

816

817

818

819

820

821

822 823

824 825

826

827 828

829

830

831

832

833

834

835

836

837

838 839

840

841

842

843

844

845

avoids degenerate cases. Rule 2 avoids redundancy in the transformations - for instance, we could have implemented an individual transformation <code>translate_up_right</code>, but this would always be equivalent to the transformation sequence <code>translate_up</code> and <code>translate_right</code>. Rule 2, however, doesn't imply that each transformation suite <code>necessarily</code> yields a unique output grid that could not have been reached with another transformation suite. For instance, for symmetric objects, applying mirror transformations could yield the same output objects as applying the rotation transformations twice - this is not the case for non-symmetric objects, thereby still satisfying Rule 2. We refer the reader to Appendix D for an evaluation of the learnibility of each of the transformations.

We summarize below all 10 families of transformations available in the generator, and a description of the available variations.

- Translate (Up, Down, Left, and Right): Translates the entire object by one pixel in any of the 4 dimensions.
- Mirror (Horizontal and Vertical): Mirrors the object with respect to the vertical or the horizontal symmetry axis.
- Rotate (90 degrees): Rotates the object by 90 degrees.
- Crop (Top Side, Bottom Side, Right Side, Left Side, Contours): Crops the object's specified side(s).
- Change Color (mod 9+1): Changes object color to new_color = original_colormod 9+1 (e.g., if the object's color is 7, it is changed to the color 8).
- Fill (Same Color, Different Color): Fills object holes with its color, or the mod 9+1 color.
- Empty: Empties inside of the object, and leaves contours.
- Extend(Same Color, Different Color): Extends the outermost edges of the object with either the same color or (mod 9+1) color.
- Pad (Top, Bottom, Left, Right, Full object): Pads in the specified direction with a fixed color.
- Duplicate (Top, Bottom, Left, Right, Quadruple): Duplicates the object in the specified direction.

C.3 COGITAO GENERATION ALGORITHM

Below is an outline pseudocode of the COGITAO generation framework.

 $\label{lem:algorithm:lem:alg$

```
1: for d in transformation depth do
       transformation_suite ← sampleTransformations(init_params, possible_transformations)
3: while trial_n < max_trials & example_n ≤ wanted_examples do
       input_grid, objects ← setInitialGrid(init_params, transform)
4:
5:
       output\_grid \leftarrow input\_grid
       for object in objects do
6:
7:
           for transformation in transformation_suite do
8:
              output grid ← transformAndPosition(output grid, object, transformation)
9:
       task \leftarrow (input\_grid, output\_grid, transformation\_suite)
10: Return: task, transform
```

The sampleTransformations () function simply iterates through the pool of transformations at the desired depth d to create the transformation sequence. An important function of our algorithm is setInitialGrid(), which sets up the randomly sampled objects in the grid given the init_params (e.g. number of objects, desired object properties) and the sampled transformation sequence. Indeed, each transformation is defined with a set of object constraints, which are object properties for which the transformation can be applied without ambiguity. This function thus ensures that the random sampling of objects aligns with the sampled transformation sequence to avoid unexpected errors. The setInitialGrid() function

positions objects to keep them fully within the grid and to avoid contact with other objects. Finally, the transformAndPosition function applies the transformations to objects and positions them back to the grid. Importantly, this function verifies that the transformed objects are still fully within grid dimension and do not collide with other objects (although adjacent contact is allowed at the transformation stage). If contact occurs, or objects go out of bounds, the entire input-output pair is discarded and generation is restarted.

For a standard 20x20 grid, with 4 objects (smaller than 6x6) and a sequence of 2 transformations applied, the average input-output pair generation time is at $0.005s\pm0.002s^5$. Some configurations are more difficult and therefore more time-consuming to generate. For instance, decreasing the grid size and increasing the number of objects can significantly increase the generation time. Some transformation combinations are also more challenging to generate, such as series of object duplications which quickly yield objects too large for the grids.

⁵These figures were obtained on an Ubuntu 22.04.5 LTS machine equipped with two AMD EPYC 7742 64-Core Processors (128 cores total) running at up to 2.25 GHz, and 256 GB of system RAM

D COGITAO TRANSFORMATIONS LEARNABILITY

To assess the learnability of each transformation introduced, we performed experiments to evaluate how effectively the models in the paper learn to apply transformations to new objects. This was conducted through a "Sample Efficiency" study, where models were given varying amounts of training data to determine the data required to master each transformation. This approach provides direct insights into 1) how easily each model learns each transformation and 2) what models are more efficient at learning given transformations. The latter idea is useful to evaluate the inductive biases of models.

For this purpose, we designed four experimental settings with different numbers of distinct training samples: 100, 1,000, 10,000, and 100,000 examples. These sample sizes were selected based on the known sample inefficiency of Transformer models. While 100 examples are generally insufficient for Transformers to learn effectively—a limitation not observed in humans—100,000 examples approach a scale where Transformers typically achieve competitive performance.

Each setting involves the same set of tasks, with each task corresponding to an elementary or atomic transformation from one of 10 distinct transformation families (e.g., the translate_up task represents the "translation" family, which also includes translate_down, translate_left, etc.). We conducted 10 experiments per setting, each focusing on a single transformation family, resulting in a comprehensive evaluation across all families. We train for 10 epochs on all experiment settings. The environment for all experiments was standardized: a fixed 15×15 grid with two objects per grid, each no larger than 6×6 . For evaluation, we tested each model on 1,000 unseen samples of the same transformation used during training, maintaining consistent environment and object parameters.

The experiments are organized into settings labeled S-x-i, where i denotes the specific transformation and x indicates the number of training samples (e.g., S-1-i for 100 samples, S-2-i for 1,000 samples, S-3-i for 10,000 samples, and S-4-i for 100,000 samples). In the below outline, we keep x to denote the varying experiment setting (and number of training samples). Below, we outline the experimental setup for the sample-efficiency study.

D.1 SAMPLE-EFFICIENCY EXPERIMENTS

- S-x-1: Train and test on the atomic transformation translate_up as a proxy for all translate transformation family.
- S-x-2: Train and test on the atomic transformation rot_90 as a proxy for all rotate transformation family.
- S-x-3: Train and test on the atomic transformation mirror_horizontal as a proxy for all mirror transformation family.
- S-x-4: Train and test on the atomic transformation extend_contours_different_color as a proxy for all extend transformation family.
- S-x-5: Train and test on the atomic transformation <code>empty_inside_pixels</code> as a proxy for all <code>empty</code> transformation family.
- S-x-6: Train and test on the atomic transformation <code>crop_top_side</code> as a proxy for all <code>crop</code> transformation family.
- S-x-7: Train and test on the atomic transformation fill_holes_different_color as a proxy for all fill transformation family.
- S-x-8: Train and test on the atomic transformation double_up as a proxy for all duplicate transformation family.
- S-x-9: Train and test on the atomic transformation change_shape_color as a proxy for all change_color transformation family.

• S-x-10: Train and test on the atomic transformation pad_shape as a proxy for all pad transformation family.

For a full list of transformations, we refer the reader back to section C.2.

In the most constrained setting (S1), all models, including the more sophisticated Transformer-based ones, completely fail to learn and generalize in-domain. All reported test accuracies being 0.0 suggests that it is likely that none of the models possess the ability to truly conceptualize simple spatial transformations in a data-scarce setting; this is unlike humans, who are able to generalize from only a few COGITAO examples. This result may reinforce the well-known *sample-inefficiency* of Deep Learning approaches, and more specifically of Transformers, as they appear to continue to rely on statistical pattern matching, which cannot easily emerge from training on only 100 samples while testing on 1000 samples of high (in-domain) diversity.

In S2, we begin to observe a divergence in model performance. The models imbued with strong inductive biases greatly increase their performance with more than an additional 50% accuracy increase. The Vanilla-TF, possessing only a weak inductive bias, achieves only 11.2%. The worse performance (19.9%) of LLaDA compared to the other Transformer-based models is possibly due to nature of its diffusion mechanism as well as the lack of a stronger inductive bias such as through the use of visual tokens.

In S3 the next order of magnitude of 10'000 training examples, all models show a marked improvement. ResNet reaches 96.1%, and Grid-TF achieves 97.1%. The P-L-TF model shows the beginning of decrease in improvement at 88.2%, while LLaDA shows a significant gain at 66.5%. Interestingly, Vanilla-TF also catches up (59.3%), but still lags behind models with stronger inductive biases. This narrowing of the performance gap indicates that Transformer-based models being to learn well past some threshold of amount of data, at which point they begin to robustly extract structures and create useful representations from symbolic grids. The fact that the Grid-TF model outperforms even the ResNet model at this scale—typically considered far smaller than Transformer data regimes—suggests a benefit of Transformer models enhanced with grid-aware tokens and relational inductive biases through object and relative positional encodings for abstract visual reasoning tasks.

In the highest data regime S4, all models reach high performance. Grid-TF nearly saturates accuracy at 99.9%, while the simpler baseline models. ResNet and Vanilla-TF, perform even better than the Pondering Looped TF and LLaDA. The greater complexity of the learning mechanism of the Pondering Looped TF and LLaDA models may partly explain why they slightly underperform compared to the other models. Moreover, the results confirm that Transformer models, even in their vanilla form, can ultimately learn atomic visual transformations when given larger-scale data.

The Sample-Efficiency table in D.1 with all the experiments also shows that some atomic transformations are more difficult to learn than others. For instance, a translation is efficiently learned while a rotation or an extension of contours appears more difficult for all the models.

Overall, the experiments demonstrate that all models are capable of learning all the atomic transformations currently offered by COGITAO. This implies that the individual tasks are not a limitation for the more involved and complex tasks of the experiments part of the other two studies of Systematic Generalization and Compositionality.

		ResNet	Vanilla-TF	Grid-TF	PL-TF	LLaDA
Setting	Transf. Family	ID	ID	ID	ID	ID
	translate	0.0	0.0	0.0	0.0	0.0
	rotate	0.0	0.0	0.0	0.0	0.0
	mirror	0.0	0.0	0.0	0.0	0.0
S1	extend	0.0	0.0	0.0	0.0	0.0
	empty	0.0	0.0	0.0	0.0	0.0
	crop	0.0	0.0	0.0	0.0	0.0
	fill	0.0	0.0	0.0	0.0	0.0
	duplicate	0.0	0.0	0.0	0.0	0.0
	change_color	0.0	0.0	0.0	0.0	0.0
	pad	0.0	0.0	0.0	0.0	0.0
	translate	100.0	0.0	100.0	83.7	78.6
	rotate	5.7	0.0	0.0	0.0	0.0
	mirror	27.4	2.3	2.9	4.6	0.1
S2	extend	32.0	0.0	16.1	23.1	0.0
	empty	100.0	9.2	100.0	80.8	8.4
	crop	97.9	0.1	94.0	84.4	34.0
	fill	100.0	0.0	98.1	82.6	6.2
	duplicate	16.4	0.0	0.2	19.7	0.0
	change_color	100.0	100.0	100.0	100.0	79.1
	pad	97.1	0.0	95.3	89.0	0.0
	translate	100.0	100.0	100.0	100.0	99.9
	rotate	94.4	0.0	96.6	88.0	28.1
	mirror	98.3	3.8	97.0	82.6	50.8
S3	extend	95.8	36.6	80.3	79.9	28.5
33	empty	100.0	91.2	100.0	99.5	97.7
	crop	99.6	90.5	98.8	89.0	95.9
	fill	100.0	67.8	99.9	79.2	94.9
	duplicate	72.9	13.5	98.6	84.8	65.1
	change_color	100.0	100.0	100.0	100.0	99.9
	pad	100.0	89.6	100.0	79.5	94.0
	translate	100.0	100.0	100.0	99.4	100.0
		99.7	96.9	99.8	98.5	99.0
	rotate					
64	mirror	99.8	98.8	100.0	99.1	98.9
S4	extend	100.0	95.9	99.4	79.8	90.5
	empty	100.0	99.9	100.0	100.0	99.9
	crop	100.0	99.3	100.0	99.7	99.9
	fill	100.0	99.6	100.0	87.4	99.9
	duplicate	86.3	99.1	100.0	91.7	97.8
	change_color	100.0	100.0	100.0	100.0	100.0
	pad	100.0	100.0	100.0	82.2	100.0

Table 2: In-domain (ID) test grid accuracy for the Sample-Efficiency settings S1–S4, across the models ResNet, Vanilla-TF, Grid-TF, PL-TF and LLaDA for each transformation family. S1 trains with 100 samples, S2 trains with 1,000 samples, S3 trains with 10,000 samples, and S4 trains with 100,000 samples.

E EXPERIMENT DETAILS

We designed our benchmark experiment to exemplify the use of our generator, and show how state-of-the-art vision models still consistently fail at such elementary tasks as they require compositionality. We provide in this appendix further details into each experiment.

Compositional Generalization Study (CompGen) For all *CompGen* study, we fix the number of objects to 2, the grid size to 20x20, the object dimension to be smaller or equal to 6x6, and all objects to be fully connected (no unconnected parts - see C.1 "Connectivity"). For each CompGen experiment setting, we generate 100000 training samples, 1000 in-distribution validation samples, 1000 out-of-distribution (OOD) validation samples, 1000 test samples, and 1000 OOD test samples. The results we report are based on the two aforementioned test sets. Based on these parameters, we then design all experiment settings in such a way that the training and testing sets are built from different "transformation sequences" (i.e. sequence of transformations). In the CompGen study, the transformation sequence varies within and between data samples. We thus provide the model with information on which transformation sequence it must apply by appending a task code to the input sequence. The task code is a sequence of tokens that indicates to the model the transformations it must apply (in the correct order). To account for varying "depth" of transformation sequence, we simply pad the input sequence with "identity transformation" tokens - as such, we always append a task code of depth 4 - which is the maximum depth of transformation sequence we consider in the entirety of our experiments. We chose the transformations sequences to be from different transformation families, and to be easily composable with one another within the constrained object and grid dimensions. Below is a detailed summary of our experiment settings and experiments.

- C1 From Restricted Composite Tasks and Atomic Tasks to Unseen Composite: We train on a set of composite tasks made of some atomic transformations, and test on composite tasks of the same depth, but not seen during training
 - C1-1: Train on the atomic transformations translate_up, rotate90, mirror_horizontal and all of their mutual compositions (depth d=2), except the specific composition translate_up rotate90 (and its commutable reverse), which we leave for OOD testing.
 - C1-2: Train on the atomic transformations change_object_color, pad_right, fill_holes_different_color and all of their mutual compositions (depth d=2), except the specific composition change_object_color pad_right, which we leave for OOD testing.
 - C1-3: Train on the atomic transformations <code>crop_bottom_side</code>, <code>rotate_90</code>, <code>pad_top</code> and all of their mutual compositions (depth d=2), except the specific composition <code>rotate_90-crop_bottom_side</code>, which we leave for OOD testing.
 - C1-4: Train on the atomic transformations double_right, crop_contours, change_shape_color and all of their mutual compositions (depth d=2), except the specific composition double_right crop_contours, which we leave for OOD testing.
 - C1-5: Train on the atomic transformations extend_contours_same_color, mirror_vertical, pad_left and all of their mutual compositions (depth d=2), except the specific composition pad_left extend_contours_same_color, which we leave for OOD testing.
- C2 From Restricted Composite Tasks to Unseen Composite: We train on a set of composite tasks made of some atomic transformations, and test on composite tasks of the same depth, but not seen during training.
 - C2-1: Train on all the mutual compositions (depth d=2) of translate_up, rotate90, mirror_horizontal, except the specific composition translate_up rotate90 (and its commutable reverse), which we leave for OOD testing.

- C2-2: Train on all the mutual compositions (depth d=2) of change_object_color, pad_right, fill_holes_different_color, except the specific composition change_object_color pad_right, which we leave for OOD testing.
 - C2-3: Train on all the mutual compositions (depth d=2) of <code>crop_bottom_side</code>, <code>rotate_90</code>, <code>pad_top</code>, except the specific composition <code>rotate_90-crop_bottom_side</code>, which we leave for OOD testing.
 - C2-4: Train on the mutual compositions (depth d=2 transformations double_right, crop_contours, change_shape_color, except the specific composition double_right crop_contours, which we leave for OOD testing.
 - C2-5: Train on all the mutual compositions (depth d=2) of extend_contours_same_color, mirror_vertical, pad_left, except the specific composition pad_left extend_contours_same_color, which we leave for OOD testing.
- C3 From Composite Tasks to Deeper Composite Tasks: We train on a set of composite tasks made of some atomic transformations, and test on composite tasks with the same transformations, but with one additional level of depth.
 - C3-1: Train on all the atomic transformations and mutual compositions (depth d=2) of translate_up, rotate90, mirror_horizontal, and OOD test on all the compositions of depth d=3 of these transformations.
 - C3-2: Train on all the atomic transformations and mutual compositions (depth d=2) of change_object_color, pad_right, fill_holes_different_color, and OOD test on all the compositions of depth d=3 of these transformations..
 - C3-3: Train on all the atomic transformations and mutual compositions (depth d=2) of crop_bottom_side, rotate_90, pad_top, and OOD test on all the compositions of depth d=3 of these transformations.
 - C3-4: Train on all the atomic transformations and mutual compositions (depth d=2) of double_right, crop_contours, change_shape_color, and OOD test on all the compositions of depth d=3 of these transformations.
 - C3-5: Train on all the atomic transformations and mutual compositions (depth d=2) of extend_contours_same_color, mirror_vertical, pad_left, and OOD test on all the compositions of depth d=3 of these transformations.
- C4 From Growing Restricted Composite Tasks and Atomic Tasks to Unseen Composite: We train on a growing pool of atomic transformations and all of their single and double mutual compositions (depth d=2), and test on an unseen double composition. The hypothesis is that the more variety a model sees during training, the more it would learn to compose. Specifically, for each experiment we exclude the composition double_right-rot90 (and its commutable reverse) from the training set and reserve it for OOD testing. The transformation pool grows with each experiment:
 - C4-1: Train on mirror_horizontal, rot90, double_right and all their single/double compositions except double_right-rot90.
 - C4-2: Extend the pool to 6 transformations by adding translate_up, crop_top_side, mirror_vertical.
- C4-3: Extend to 9 transformations by further adding pad_top, translate_right, pad_right.
- C4-4: Extend to 12 transformations by adding fill_holes_same_color, fill_holes_different_color, change_shape_color.
- C4-5: Extend to 15 transformations by adding empty_inside_pixels, double_down, extend_contours_same_color.

1128 **Environment Generalization Study (EnvGen)** For each *EnvGen* experiment setting, we generate 100000 1129 training samples, 1000 in-distribution validation samples, 1000 out-of-distribution (OOD) validation samples, 1130 1000 test samples, and 1000 OOD test samples. The results we report are based on the two aforementioned 1131 test sets. For each EnvGen experiment, we fix the transformation sequence (as described below depending on 1132 the experiment) and vary some parameters, such as the grid size, the number of objects, the object dimensions 1133 or the object properties. The varying parameters constitutes what changes between the in-distribution and OOD testing sets, and forms the basis of the "generalization" experiment. As opposed to the CompGen 1134 setting, where there are multiple transformation sequences per set, we do not need to provide a task code to 1135 the model, but only a single grid on which it must perform the transformation based on the grid settings. To 1136 account for varying grid sizes in some of the experiments, we simply pad the the input sequence to the max 1137 size which can be observed during the experiment. 1138

- G1 Number of Objects Difficulty: We train on grids with 1 or 2 objects, and OOD test on grids with 3 or 4 objects. We fix the grid size to 15x15.
 - G1-1: Perform experiment with the translate up transformation.
- 1142 - G1-2: Perform experiment with the rotate 90 transformation.

1139

1140

1141

1143

1144

1145

1146

1149

1150

1151

1154

1155

1156

1160

1166

1167

1171

- G1-3: Perform experiment with the mirror_horizontal transformation.
- G1-4: Perform experiment with the crop_top_side transformation.
- G1-5: Perform experiment with the extend_contours_same_color transformation.
- G2 Grid Size Difficulty: We train on grid sizes between 10x10 and 15x15, and OOD test on grid sizes 1147 between 16x16 and 20x20. We fix the number of objects to 2. 1148
 - G2-1: Perform experiment with the translate_up transformation.
 - G2-2: Perform experiment with the rotate_90 transformation.
 - G2-3: Perform experiment with the mirror_horizontal transformation.
- G2-4: Perform experiment with the <code>crop_top_side</code> transformation. 1152
- G2-5: Perform experiment with the extend_contours_same_color transformation. 1153
 - G3 Object Dimension Difficulty. We train on grids with objects of size between 1x1 and 5x5, and OOD test on grids with objects of size between 6x6 and 10x10.
- G3-1: Perform experiment with the translate_up transformation. 1157
- G3-2: Perform experiment with the rotate_90 transformation. 1158
- G3-3: Perform experiment with the mirror_horizontal transformation. 1159
 - G3-4: Perform experiment with the crop_top_side transformation.
- G3-5: Perform experiment with the extend_contours_same_color transformation. 1161
- 1162 • G4 - Object Complexity Difficulty We train on grids with symmetric and single-colored objects, and 1163 OOD test on grids with asymmetric and multi-colored objects. We fix the number of objects to 2, the grid 1164 size to 15x15, and the object dimension to smaller than 6x6. 1165
 - G4-1: Perform experiment with the translate up transformation.
 - G4-2: Perform experiment with the rotate_90 transformation.
 - G4-3: Perform experiment with the mirror horizontal transformation.
 - G4-4: Perform experiment with the crop_top_side transformation.
- 1169 - G4-5: Perform experiment with the extend_contours_same_color transformation. 1170
- G5 All Difficulties Combined We train on grids with symmetric, single-colored objects of size between 1172 1x1 and 5x5, with 1 or 2 objects, and grid sizes between 10x10 and 15x15. We OOD test on grids with asymmetric, multi-colored objects of size between 6x6 and 10x10, with 3 or 4 objects, and grid sizes between 16x16 and 20x20.

- G5-1: Perform experiment with the translate_up transformation. - G5-2: Perform experiment with the rotate_90 transformation. - G5-3: Perform experiment with the mirror_horizontal transformation. - G5-4: Perform experiment with the <code>crop_top_side</code> transformation. - G5-5: Perform experiment with the extend_contours_same_color transformation.

F Models

The selection of encoder networks includes both standard baselines (ResNet, Vanilla TF) and more specialized architectures (Grid TF, Pondering Looped TF, LLaDA) designed to better capture abstract and spatial reasoning, compositionality, and generalization capabilities.

Table 3 summarizes some of the notable architectural and modeling characteristics used for each encoder network part of the models. The models were designed to roughly have the same size of 1.2 Million of parameters in order to propose a fairer performance comparison, in spite of being aware that different architectures may have different modeling requirements to optimize their performance.

Table 3: Overview of the encoder networks for the different architectural and modeling techniques considered. APE: Absolute Positional Encoding. OPE: Object Positional Encoding. RPE: Relative Positional Encoding. VT: Visual Tokens. Registers: Register tokens. PEMixer: Positional Encoding Mixer, where "vec weighted sum" signifies a vector-weighted sum.

		Architectural							
Encoder	APE	RPE	PEMixer	Recurrence	Diffusion	VT	Registers		
ResNet	_	_	_	_	_	_	_		
Vanilla-TF	learned	_	sum	_	_	—	_		
Grid-TF	2D-sincos w/OPE	RoPE	vec weighted sum	_	_	\checkmark	\checkmark		
PL-TF	2D-sincos	RoPE	sum	\checkmark	_	\checkmark	_		
LLaDA	_	RoPE	_	_	\checkmark	\checkmark	_		

F.1 RESNET

We employ an architecture based on ResNet(27) as a standard baseline notable for its strong historical performances on vision tasks, principally distinguishing itself from the other models evaluated here by its convolutional inductive bias and lack of attention mechanism.

In our implementation, the input grid is processed as a low-resolution image after an artificial channel dimension is created through one-hot encoding of the token categories that can possibly be predicted (i.e., num_token_categories). Then, the core of the encoder consists of a sequence of residual blocks. Crucially, all convolutional operations within these blocks are performed without any spatial downsampling (e.g., using stride 1 convolutions and no pooling layers). Despite missing on a slightly more global receptive field, this design choice is important for our tasks, as it strictly preserves the spatial dimensions of the feature maps throughout the network and thus does not require an approach of upsampling. The stacking of convolutional layers without downsampling should also allow the effective receptive field for each individual output pixel to grow, enabling the model to better capture useful context regions while retaining more precise spatial information.

Our specific ResNet architecture comprises:

- An initial convolutional layer to project the input grid channels to the model's hidden dimension: num_token_categories input channels, 32 output channels, kernel size of 1, stride of 1, padding of 0. This is followed by Batch Normalization (57) and a ReLU activation function (58).
- A series of 5 residual blocks:
 - 1. 32 input channels, 64 output channels, kernel size of 3, stride of 1, padding of 1.
 - 2. 64 input channels, 128 output channels, kernel size of 3, stride of 1, padding of 1.

- 3. 128 input channels, 128 output channels, kernel size of 1, stride of 1, padding of 0.
 - 4. 128 input channels, 256 output channels, kernel size of 3, stride of 1, padding of 1.
 - 5. 256 input channels, 128 output channels, kernel size of 1, stride of 1, padding of 0.
 - A final convolutional layer (1x1 convolution) to map the features from the last residual block to the required embed dimension per pixel/token: 128 input channels, embed_dim output channels, kernel size of 1, stride of 1, padding of 0.

F.2 VANILLA TF

We adapt the standard Vision Transformer architecture, as defined in (46), to our grid-based tasks. The (padded and one-hot encoded) input grid is divided into a sequence of non-overlapping patches, which are effectively single tokens since we use a patch size and stride of 1 when linearly projecting the grid image into the embedding dimension using a 2D convolution.

A basic approach to incorporate spatial information is to use (randomly initialized) 1D learnable positional embeddings to add to the embedded input sequence before it is passed to the encoder network.

This vanilla Transformer encoder consists of multiple layers, each containing a multi-head self-attention (MHSA) mechanism followed by a position-wise feed-forward network. We use Pre-Layer Normalization (Pre-LN) (59)(60) and thus apply Layer Normalization before both the MHSA and feed-forward sub-layers. Residual connections are also used around each sub-layer, as is standard. To be able to produce the output grid using an MLP head, a linear layer is applied to each output token of the sequence (from which the special extra tokens have been truncated) at the end of the encoder network in order to map the embedding dimension to that of the MLP head which will then predict the logits for all of the tokens which, once softmax applied and spatially reshaped, form the output grid.

Notable hyperparameters are:

- Input grid partitioning: Patch size of 1, stride of 1. The grid is partitioned at the pixel-level.
- Embedding dimension: 128.
- Number of encoder layers: 6.
- Number of attention heads in MHSA: 4.
 - Dimensionality of the feed-forward layer: Factor of 4 times the embedding dimension, thus 512.
- Activation Functions: GELU (61).
 - Output projection: A linear layer maps each embed_dim-dimensional output token (excluding the extra tokens such as the register tokens or the task embedding) to num_classes logits, where num_classes depends on the number of tokens to predict (e.g., 15 if Visual Tokens are used, 11 otherwise, as there are ten for the 0-9 symbols and one for padding).

F.3 GRID TF

The Grid-TF is a variant of the Vision Transformer architecture adapted to improve performance on abstract visual reasoning tasks, especially in grid-like environments, similar to the COGITAO data. It incorporates several modifications to improve spatial and abstract visual reasoning. Similar to the Vanilla TF, the input grid is embedded as patches at the pixel level (i.e., patch size and stride of 1 when performing the 2D convolution to transform the grid into an embedded sequence).

The key architectural modifications from the Vanilla-TF are:

Positional Encodings:

1318

1319

1320 1321

1322

1323

1324

1325 1326

1327

1328

1329

1330 1331

1332

1333

1334

1335

1336 1337

1338

1339

1340

1342

1343 1344

1345

1346

1347 1348 1349

1350

1351

1352 1353

1354

1355

1356

1357

1358

1359

1360

1361

1362

- 1316 - 2D Absolute Positional Encoding (APE): We use 2D sinusoidal absolute positional encodings, extended from the 1D sinusoidal absolute positional encodings used in (47), which are fixed (i.e., not learned) and directly reflect the 2D nature of the input grid. They are added to the patch embeddings following the PEMixer strategy.
 - Object Positional Encoding (OPE): OPE is used as part of the APE, as described in (26) where half of the APE dimension is allocated to the object positions while the other half is used for the x and y positions in the grid. The OPE is also typically coupled with an appropriate PEMixer strategy, such as a vector-weighted sum. We make the choice to compute the object positions after having padded (whether with Visual Tokens or with simple padding) the input grid, as opposed to before.
 - Positional Encoding Mixer (PEMixer): The PEMixer presented in (26) defines the strategy by which we encode the absolute positional information into the input embeddings from the absolute positional embeddings. It allows different strategies such as a sum (the standard one), a weighted sum, a vectorweighted sum, etc.
 - Relative Positional Encoding (RPE): Due to the importance of the relative positions of the grid tokens when transforming objects, an RPE scheme comes in as a natural consideration. Among possible techniques of RPE, we choose to use Rotary Position Embedding (RoPE) (50), incorporated into the self-attention mechanism in order to inject relative spatial information between the grid tokens. After initial experiments with ALiBi (62), another RPE method, extended to 2D as in (26), we found that RoPE yields comparable performance on our tasks and thus decided to use RoPE for its simplicity.
 - Registers: We prepend (6) register tokens to the input sequence, following results from (48) and a drawn parallel to slots for object-centric learning in (63). Those registers are additional, randomly initialized and learnable tokens appended to the sequence of patch embeddings in order to possibly improve model performance by functioning as containers for less informative "background" regions of the grid. Thus, they do not correspond to any specific input informing the model and should be leveraged by the attention mechanism to improve global context aggregation and internal representations. The positional encodings are not used for those extra tokens.

Another modification to the Vanilla-TF is the use of dropout. We apply dropout with a rate of 0.1 after the multi-head self-attention layer and after the feed-forward layer in each Transformer encoder block.

The remaining notable hyperparameters are the same as for the Vanilla-TF.

F.4 PONDERING LOOPED TF (PL-TF)

The Pondering Looped Transformer model closely follows the PonderNet paper by Banino et al. (24), using a looped Transformer with weight-sharing as the encoder.

The PL-TF fundamentally differs from the other transformer models in two aspects:

- It possesses an inductive bias of recurrent architecture leveraging weight-sharing through an iterative looping process over the same block structure (25; 64; 65; 66). At each step, the model updates the latent representation, which can be useful to mimic a multi-stage reasoning process for tasks that require multiple sequential operations on objects.
- It makes use of a carefully designed adaptive compute time framework–named PonderNet–controlling the number of iterations and computation effort spent on each data sample (24). Essentially, the model learns a halting probability at each iterative step from an aggregated representation of the current hidden state, which allows it to dynamically and probabilistically decide the number of iterations needed for a given input.

Since parameter-efficiency is not a primary goal, in order to obtain a learnable parameter count comparable to that of the other models, the embedding dimension is set to $d_{model} = 256$ -instead of $d_{model} = 128$ as in the other transformers—and the number of attention heads is set to eight. We use a single encoder block (although more can be used) with weight-sharing.

The computational resource constraints led to the setting of a relatively low maximum number of pondering steps, although a larger maximum number of steps is likely required to fully harness the capabilities of the recurrent and pondering modules. We note that with those decisions the total number of passes through an encoder block is not too far off from that of the other transformers. Furthermore, the pondering-specifc hyperparameters used are: 2-layer halting node with hidden dimension of 128, ϵ of 0.01, λ_p of 0.05, β of

The encoder block is the same as the Grid-TF with pre-LN, additive skip connections, dropout of 0.1 and a RoPE RPE scheme in the MHSA module. The PL-TF leverages Visual Tokens as the Grid-TF but it uses a 2D sincos APE scheme without object positional encoding or PEMixer.

F.5 LLADA

We include LLaDA (23) in our set of models due to its demonstrated strength on logical and arithmetic tasks. LLaDA operates non-autoregressively and exploits bidirectional dependencies over masked target sequences, making it well-suited for structured input-output mappings. We adapt the original LLaDA setup skipping pretraining and training it from scratch via supervised learning. Each instance of input data is represented as a flattened concatenation of a task embedding, input sequence, and a partially masked target sequence. During training, a random portion of target tokens is masked (mask ratio sampled uniformly in [0, 1]), and the model is trained to reconstruct the masked tokens. At inference, the target is fully masked, and reconstruction proceeds over 32 denoising steps, each resolving a fraction of the masked tokens based on confidence.

In contrast to the original architecture, We use a lightweight 6-layer version with approximately 1.3M parameters. The architecture uses an embedding dimension of 128, a feedforward hidden size of 384 (MLP ratio of 4), and 4 attention heads. The model incorporates RMSNorm (67) with affine parameters and uses SiLU activation functions (68). Rotary positional embeddings (RoPE) (50) are applied independently within each transformer layer, using a shared base frequency parameter of $\theta = 500,000$. Weights are initialized via the Mitchell method with a standard deviation of 0.02. No dropout is used throughout training. The model's vocabulary comprises 12 tokens, reflecting the tokenized representation used in COGITAO, and includes special tokens for padding and masking.

G TRAINING PROCEDURE

To ensure a fairer comparison across different models, we adopted a consistent training and evaluation framework whenever possible. Key aspects are detailed as follows:

• Training Procedure and Data: All models were trained from scratch using supervised learning. We used a dataset of 100'000 unique samples. Training proceeded for 10 epochs with a batch size of 64, meaning each model saw a total of 1'000'000 samples, This implies a sample-efficient mode of experimentation, as observed through the training learning curves hinting at a non-terminal convergence for several experiments and considering the typical quantity of samples that Transformer-based models require.

• Validation and Testing: Model performance was monitored during training on a validation set of 1'000 samples. After training, models were evaluated on a distinct held-out test set of 1'000 samples. We always compute the performance on ID *and* OOD val/test sets.

• Modeling Strategy:

- An input grid with shape [H, W] is converted to an artificial image of shape [C, H, W] by the creation of a channel dimension through one-hot encoding of the categories of tokens that can be predicted.

- For the experiments within the CompGen study, the transformations sequence vary within the trainin set (and w.r.t. the OOD sets). We therefore provide the model with some context in the form of a task embedding in order to inform it of what task it should perform given the input grid. For that purpose, we considered two approaches: task tokens and in-context example. We decided to use the first approach, where we provide the model with a sequence of tokens representing the atomic transformations composing the task to perform. The second approach was to provide the model with an example (i.e., an input-output pair of grids) of the task to perform. However, it was not experimented with due to time and resource constraints.

• Early Stopping and Model Selection: No early stopping was performed as the number of epochs was restricted and in most experiments the models showed steady convergence throughout the 10 epochs. The checkpoint used for final testing was chosen based on the best (lowest) validation loss achieved on the OOD validation set.

• Loss Function: We employed a pixel-wise cross-entropy loss, calculated between the entire predicted token grid and the ground-truth target grid, both padded to a maximum size equal to the largest grid size within the dataset.

• Evaluation Metric: The primary metric for reporting performance is grid accuracy. This is the percentage of predicted grids that perfectly match the ground-truth target grids. Both grids were padded to the maximum grid size observed in the dataset before comparison. The padding is either composing of usual padding tokens or of special padding tokens named "Visual Tokens" (VTs)(26). This means that when VTs are used as part of the modeling strategy for Transformer-based models, the model has to predict correctly the whole padded grid, with its special padding tokens, in order to perform well since the metric computation does not discard the tokens/pixels outside of the boundaries denoted by the true grid size.

• Optimizer and Learning Rate: The AdamW optimizer (51) was used, with a learning rate following a Cosine Annealing schedule that monitors the OOD validation loss at each epoch.

Weight Initialization: Model weights were initialized from a truncated normal distribution.

- Training Precision: Training was conducted using FP16 mixed precision.
 - Training Duration: A training run lasted between 7 minutes and 1 hour depending on the model, hardware and specific experiment.

G.1 RESNET

The learning rate and weight decay used for ResNet are of 1e-3, same as for the Vanilla-TF and Grid-TF models.

ResNet is trained without Visual Tokens, as their purpose is mainly to mitigate the loss of the 2D spatial structure when going from a 2D grid to a flattened sequence, as it is the case for Transformer models, as well as defining more explicit grid boundaries.

For the Compositionality experiments, the task embedding is appended (along the spatial dimension) to the spatially flattened output of the ResNet encoder network. This means that the task embedding only enters the input transformation process at a late stage, similar to what is done in (13), compared to how the task embedding is used with the Transformer-based models working with sequences. Practically, it is the MLP head that has to leverage the information provided by the task embedding in order to make better-informed predictions.

G.2 VANILLA-TF & GRID-TF

The two transformer models use exactly the same hyperparameters. The learning rate and weight decay are 1e-3. Before the initial learning rate is set to change with the Cosine Annealing schedule, a linear warm-up phase takes place for 200 steps.

A key difference between the Vanilla-TF and the Grid-TF is that the latter uses Visual Tokens while the former does not.

The input sequence to the transformer results from the one-hot encoding of the input grid for which embedding patches are created using a 2D convolution with patch size of 1 and stride of 1.

For the Compositionality experiments, the task embedding is appended (along the spatial dimension) to the input sequence *before* being encoded by the ViT. This provides the full task context at the start of the processing of the input by the model, thus increasing the information about the task to perform propagated through the model.

G.3 PONDERING LOOPED TF

The PL-TF is trained similarly to the two previous transformer models and follows the PonderNet paper (e.g., with regard to the update of the reconstruction and regularization losses). It mainly uses the same hyperparameters as the aforementioned models, but with a smaller batch size of 32 due to the possible increase in computations and resource constraints. It uses data modeled with Visual Tokens as for the Grid-TF.

G.4 LLADA

We train the LLaDA model using the same hyperparameter configuration as that employed for the vision transformer baselines, including the Vanilla ViT and Grid ViT architectures. However, we introduce two key modifications: Firstly, while retaining the AdamW optimizer (51), we reduce the learning rate to 2×10^{-4} and set the weight decay to 0.01. Empirically, this lower learning rate leads to significantly faster convergence for LLaDA during training. Second, we extend the training schedule to 20 epochs, doubling the number

of training epochs compared to the baseline setup. This adjustment compensates for the fact that LLaDA masks only approximately 50% of the target tokens on average, thereby ensuring that all models are trained to predict a comparable total number of tokens and enabling a fair evaluation.

RESULTS Η

1551

1552 1553

1554

1555

1556

1557

1558

1560

1561 1562

1563

1564

1565

1566

1567

1568

1569 1570

1571

1572

1573

1574

1575

1576

1577

1578

1579

1580

1581

1582

1583

1584

1585

1586

1587

1588

1589

1590

1591

1592

1593

We present a set of results for each model and each of the 40 individual experiments considered in the studies of CompGen and EnvGen. The results reported are the average of three runs with different random seeds. A few experiments showed a high sensitivity to the random seed, up to a 15% difference, while the others yielded similar results for different runs. Tables H H H H display the in-domain (ID) and out-of-domain (OOD) test grid accuracies (i.e., the predicted grid and the ground-truth target grid, both padded to a max. size, should perfectly match) for all models considered across all the experiment settings (i.e., C1-C3 and G1-G5). While the main paper provides a summary in the form of averaged results over each setting for clarity and space constraints, the exhaustive results here enable a more granular understanding of model behavior given different transformations and compositions thereof.

We include here results of a ResNet-like model baseline, which is omitted from the main text table and discussion. As a standard convolutional neural network performing well on vision tasks - even when it includes a level of reasoning (13), ResNet is poorly designed for compositionality tasks, and is more sample efficient than Transformer-based architectures (13). Consequently, it was not deemed to be of focus in this paper, alth-ough it could provide few insights. Its inclusion here also serves to put into perspective the performance of models with clearly different inductive biases. In the main paper, we focus on models better designed for abstraction and generalization, with a Vanilla-TF as starting point, followed by Grid-TF, PL-TF and LLaDA models.

The results clearly highlight that compositional generalization remains a major challenge, which COGITAO allows to explore. Across most CompGen experiments, models perform poorly in the OOD setting. Notably, some transformations stand out as yielding easier or more difficult tasks. For example, translate up is by far the easier transformation followed for example by extend_contours_same and crop_top_side. More difficult transformations include mirror_horizontal and rotate90 which empirically, but also intuitively, are seen to be more complex. A transformation such as crop_top_side may be easier as it mainly introduces localized changes, allowing models, especially those with strong inductive biases for locality, to generalize more effectively. In contrast, transformations such as mirror_horizontal and rotate 90 result in drastic spatial reconfigurations of visual features, which can severely disrupt learned representations, in particular when not explicitly trained on such variations.

In the EnvGen experiments, ResNet performed competitively, and even better for settings focused on changes of grid size and number of objects. These experiments involve systematic variations of properties of the grid environment and scene (e.g., the grid size, the number of objects, their spatial distribution) which can still be captured through localized pixel/symbol statistics and spatial patterns that do not require compositional abilities. ResNet's strong performance here could be attributed to its architectural inductive biases: overlapping receptive fields, translation invariance from convolutions, and the ability to encode detailed local structures without aggressive downsampling (as per our implementation). We suspect that these properties enable it to effectively maintain useful representations when the domain shift involves more spatially coherent variations, as opposed to more abstract ones based on a compositional prior.

These detailed tables serve not only as a complement to the averaged results in the main paper, but also as a valuable diagnostic tool for evaluating the specific generalization challenges posed by different transformations. They reinforce the necessity of designing models and training regimes that can robustly handle a wide range of compositional and systematic shifts in visual input with respect to diverse transformations implying fundamentally different types of changes in the grid. Consequently, an exhaustive table with more experiments for all the transformations enabled by COGITAO would be a natural extension of those results.

		Res	Net	Vanil	la-TF
Setting	Experiment	ID	OOD	ID	OOD
	experiment-1	0.1 ± 0.1	0.0 ± 0.0	23.3 ± 5.6	0.0 ± 0.0
C1	experiment-2	8.9 ± 3.1	0.0 ± 0.0	22.7 ± 3.1	0.0 ± 0.0
CI	experiment-3	1.0 ± 0.1	0.0 ± 0.0	5.4 ± 0.7	0.0 ± 0.0
	experiment-4	2.3 ± 0.9	0.0 ± 0.0	16.7 ± 5.3	0.0 ± 0.0
	experiment-5	0.6 ± 0.3	0.0 ± 0.0	14.4 ± 0.4	0.0 ± 0.0
	experiment-1	0.7 ± 0.2	0.0 ± 0.0	26.8 ± 0.5	0.0 ± 0.0
C2	experiment-2	12.2 ± 6.5	0.0 ± 0.0	14.6 ± 0.5	0.0 ± 0.0
02	experiment-3	0.6 ± 0.2	0.0 ± 0.0	8.8 ± 1.2	0.0 ± 0.0
	experiment-4	7.7 ± 2.0	0.0 ± 0.0	17.3 ± 0.3	0.0 ± 0.0
	experiment-5	0.2 ± 0.1	0.0 ± 0.0	21.6 ± 1.5	0.0 ± 0.0
	experiment-1	0.0 ± 0.0	0.0 ± 0.0	13.8 ± 1.2	0.8 ± 0.1
C3	experiment-2	10.4 ± 3.2	3.2 ± 1.1	37.4 ± 5.8	5.5 ± 2.1
	experiment-3	3.0 ± 0.6	0.1 ± 0.0	12.6 ± 2.0	1.1 ± 0.3
	experiment-4	0.7 ± 0.3	0.0 ± 0.0	68.3 ± 8.1	12.3 ± 3.3
	experiment-5	0.1 ± 0.1	0.0 ± 0.0	15.1 ± 6.1	0.3 ± 0.1

Table 4: ID and OOD test grid accuracy with SEM (Standard Error of the Mean) for the *CompGen* experiments (C1–C3) across the models ResNet and Vanilla-TF.

		Grid	-TF	PL-	TF	LLaDA		
Setting	Experiment	ID	OOD	ID	OOD	ID	OOD	
	experiment-1	43.5 ± 16.9	0.0 ± 0.0	65.8 ± 1.0	0.3 ± 0.2	27.7 ± 1.4	0.0 ± 0.0	
C1	experiment-2	47.2 ± 18.6	0.0 ± 0.0	82.8 ± 0.6	0.0 ± 0.0	67.0 ± 0.4	0.0 ± 0.0	
CI	experiment-3	56.7 ± 7.7	0.0 ± 0.0	83.7 ± 1.3	0.0 ± 0.0	33.3 ± 2.5	0.0 ± 0.0	
	experiment-4	91.7 ± 0.3	0.0 ± 0.0	89.0 ± 1.5	0.0 ± 0.0	64.0 ± 29.1	0.0 ± 0.0	
	experiment-5	59.7 ± 11.9	0.0 ± 0.0	83.7 ± 0.5	0.0 ± 0.0	32.6 ± 7.5	0.0 ± 0.0	
	experiment-1	56.2 ± 5.8	0.0 ± 0.0	59.3 ± 1.0	0.5 ± 0.5	31.2 ± 0.8	0.0 ± 0.0	
C2	experiment-2	94.3 ± 1.5	0.0 ± 0.0	76.1 ± 12.8	0.0 ± 0.0	72.0 ± 1.2	0.0 ± 0.0	
C2	experiment-3	56.6 ± 5.8	0.0 ± 0.0	87.4 ± 0.7	0.0 ± 0.0	27.2 ± 1.2	0.0 ± 0.0	
	experiment-4	92.3 ± 2.2	0.0 ± 0.0	86.3 ± 3.5	0.0 ± 0.0	68.3 ± 22.6	0.0 ± 0.0	
	experiment-5	42.9 ± 9.6	0.0 ± 0.0	86.1 ± 1.0	0.0 ± 0.0	32.2 ± 3.6	0.0 ± 0.0	
	experiment-1	40.5 ± 18.8	1.2 ± 0.5	85.1 ± 1.6	1.8 ± 0.1	91.7 ± 3.3	1.2 ± 0.1	
C3	experiment-2	68.1 ± 29.5	15.0 ± 7.5	79.0 ± 4.7	19.8 ± 1.8	98.4 ± 0.6	24.5 ± 1.1	
CJ	experiment-3	51.4 ± 1.2	2.6 ± 0.4	77.5 ± 3.2	2.6 ± 0.3	82.7 ± 5.9	5.5 ± 0.8	
	experiment-4	89.7 ± 8.9	22.0 ± 4.7	85.3 ± 1.5	11.3 ± 1.5	63.3 ± 10.3	6.0 ± 4.6	
	experiment-5	66.7 ± 14.1	0.6 ± 0.3	82.9 ± 3.2	0.5 ± 0.0	84.3 ± 9.9	1.8 ± 0.7	

Table 5: ID and OOD test grid accuracy with SEM (Standard Error of the Mean) for the *CompGen* experiments (C1–C3) across the models Grid-TF, PL-TF, and LLaDA.

		Re	sNet	Vani	lla-TF
Setting	Experiment	ID	OOD	ID	001
	experiment-1	100.0 ± 0.0	100.0 ± 0.0	100.0 ± 0.0	$100.0 \pm$
G1	experiment-2	99.8 ± 0.0	96.5 ± 0.1	97.3 ± 0.2	$55.4 \pm$
01	experiment-3	99.8 ± 0.1	98.5 ± 0.2	97.5 ± 0.6	$77.5 \pm$
	experiment-4	100.0 ± 0.0	99.9 ± 0.0	98.9 ± 0.6	$77.9 \pm$
	experiment-5	99.9 ± 0.1	99.3 ± 0.1	98.2 ± 0.3	$83.7 \pm$
	experiment-1	100.0 ± 0.0	99.9 ± 0.1	98.7 ± 0.3	1.9 ±
G2	experiment-2	88.9 ± 1.3	78.2 ± 7.2	57.1 ±21.5	0.2 ±
02	experiment-3	99.3 ± 0.3	98.2 ± 0.8	81.1 ±1.3	8.2 ±
	experiment-4	100.0 ± 0.0	100.0 ± 0.0	96.3 ± 1.5	0.0 ±
	experiment-5	100.0 ± 0.0	100.0 ± 0.0	76.9 ± 2.3	0.2 ±
	experiment-1	100.0 ± 0.0	100.0 ± 0.0	100.0 ± 0.0	$88.6 \pm$
G3	experiment-2	93.7 ± 0.5	0.0 ± 0.0	0.0 ± 0.0	0.0 ±
G5	experiment-3	96.2 ± 1.9	0.1 ± 0.1	2.3 ± 0.3	0.1 ±
	experiment-4	98.9 ± 1.0	0.0 ± 0.0	93.0 ± 2.2	0.0 ±
	experiment-5	99.4 ± 0.0	35.3 ± 2.7	92.6 ± 1.4	$23.8 \pm$
	experiment-1	100.0 ± 0.0	23.7 ± 5.8	100.0 ± 0.0	90.6 ±
G4	experiment-2	30.7 ± 1.2	0.0 ± 0.0	3.8 ± 2.9	0.0 ±
J.	experiment-3	58.8 ± 2.9	0.1 ± 0.1	14.8 ± 1.0	$0.0 \pm$
	experiment-4	95.2 ± 0.6	64.1 ± 4.0	51.9 ± 2.8	$9.0 \pm$
	experiment-5	97.1 ± 0.9	36.9 ± 0.5	60.4 ±14.7	$9.4 \pm$
	experiment-1	100.0 ± 0.0	9.1 ± 2.0	97.7 ± 0.2	$0.0 \pm$
G5	experiment-2	98.3 ± 0.3	0.0 ± 0.0	91.9 ± 3.3	$0.0 \pm$
	experiment-3	98.3 ± 0.6	0.0 ± 0.0	32.7 ± 14.5	$0.0 \pm$
	experiment-4	100.0 ± 0.0	0.0 ± 0.0	98.3 ± 0.9	$0.0 \pm$
	experiment-5	99.7 ± 0.2	0.6 ± 0.2	41.9 ± 18.4	0.0 ±

Table 6: ID and OOD test grid accuracy with SEM (Standard Error of the Mean) as error bars for the *EnvGen* experiments (G1–G5) across the models ResNet and Vanilla-TF.

		Grie	d-TF	PL	-TF	LLaDA		
Setting	Experiment	ID	OOD	ID	OOD	ID	OOD	
	experiment-1	100.0 ± 0.0	100.0 ± 0.0	100.0 ± 0.0	99.9 ± 0.1	100.0 ± 0.0	99.9 ± 0.1	
G1	experiment-2	99.7 ± 0.0	92.7 ± 1.3	90.2 ± 5.0	90.0 ± 4.2	99.0 ± 0.3	83.5 ± 3.6	
G1	experiment-3	99.8 ± 0.1	95.3 ± 0.4	84.1 ± 1.7	82.0 ± 1.4	99.1 ± 0.1	84.2 ± 2.6	
	experiment-4	99.2 ± 0.1	88.5 ± 2.5	96.7 ± 1.3	72.5 ± 9.6	99.6 ± 0.0	88.9 ± 1.4	
	experiment-5	97.8 ± 0.5	73.9 ± 4.9	98.0 ± 0.8	82.9 ± 2.2	99.8 ± 0.1	94.1 ± 1.5	
	experiment-1	100.0 ± 0.0	90.5 ± 4.9	100.0 ± 0.0	38.4 ± 11.2	100.0 ± 0.0	60.6 ± 6.6	
G2	experiment-2	97.1 ± 1.8	68.5 ± 3.6	96.4 ± 3.4	75.9 ± 2.8	95.5 ± 1.3	45.3 ± 3.4	
0-	experiment-3	97.9 ± 2.1	90.6 ± 5.8	85.7 ± 7.3	65.4 ± 17.3	97.7 ± 1.8	47.8 ± 16.8	
	experiment-4	99.5 ± 0.2	94.2 ± 1.1	98.5 ± 1.1	67.2 ± 5.0	99.7 ± 0.1	89.7 ± 1.2	
	experiment-5	95.6 ± 1.1	41.4 ± 6.2	82.2 ± 4.1	27.7 ± 6.1	99.6 ± 0.2	68.7 ± 7.8	
	experiment-1	100.0 ± 0.0	99.7 ± 0.3	100.0 ± 0.0	100.0 ± 0.0	100.0 ± 0.0	99.1 ± 0.5	
G3	experiment-2	33.4 ± 33.2	0.0 ± 0.0	90.0 ± 1.1	0.0 ± 0.0	18.8 ± 18.5	0.0 ± 0.0	
	experiment-3	97.5 ± 0.3	0.1 ± 0.0	83.1 ± 10.9	0.1 ± 0.1	96.8 ± 0.6	0.1 ± 0.1	
	experiment-4	98.2 ± 1.0	0.0 ± 0.0	98.4 ± 0.6	0.0 ± 0.0	97.2 ± 1.3	0.0 ± 0.0	
	experiment-5	95.7 ± 1.4	33.1 ± 2.4	88.3 ± 5.8	35.9 ± 3.1	99.2 ± 0.5	34.7 ± 0.8	
	experiment-1	100.0 ± 0.0	79.4 ± 9.2	100.0 ± 0.0	100.0 ± 0.0	100.0 ± 0.0	99.6 ± 0.3	
G4	experiment-2	79.6 ± 5.2	0.0 ± 0.0	87.5 ± 1.4	0.1 ± 0.1	28.3 ± 28.2	0.0 ± 0.0	
	experiment-3	61.8 ± 30.9	0.0 ± 0.0	86.0 ± 0.7	19.3 ± 4.2	88.5 ± 3.6	0.9 ± 0.2	
	experiment-4	97.0 ± 1.0	15.2 ± 6.3	82.3 ± 0.4	35.8 ± 3.5	91.6 ± 2.2	24.7 ± 2.9	
	experiment-5	96.0 ± 0.8	0.1 ± 0.1	78.0 ± 10.3	32.3 ± 10.0	98.3 ± 0.7	34.7 ± 6.7	
	experiment-1	100.0 ± 0.0	1.1 ± 0.5	100.0 ± 0.0	44.4 ± 12.7	99.9 ± 0.1	50.4 ± 11.1	
G5	experiment-2	77.8 ± 13.6	0.0 ± 0.0	57.8 ± 25.9	0.0 ± 0.0	12.6 ± 8.3	0.0 ± 0.0	
	experiment-3	98.8 ± 0.4	0.0 ± 0.0	56.0 ± 25.7	0.0 ± 0.0	43.3 ± 10.3	0.0 ± 0.0	
	experiment-4	100.0 ± 0.0	0.0 ± 0.0	98.1 ± 0.8	0.0 ± 0.0	95.0 ± 1.4	0.0 ± 0.0	
	experiment-5	98.3 ± 0.5	0.0 ± 0.0	91.6 ± 0.4	0.0 ± 0.0	99.3 ± 0.4	0.0 ± 0.0	

Table 7: ID and OOD test grid accuracy with SEM (Standard Error of the Mean) for the *EnvGen* experiments (G1–G5) across the models Grid-TF, PL-TF, and LLaDA.